PEDIATRICS INTERNATIONAL Official Journal of the Japan Pediatric Society

Pediatrics International (2014) **56**, 159–166 doi: 10.1111/ped.12314

Review Article

Current research on chronic active Epstein–Barr virus infection in Japan

Shigeyoshi Fujiwara,[1] Hiroshi Kimura,[5] Ken-ichi Imadome,[1] Ayako Arai,[2] Eiichi Kodama,[6] Tomohiro Morio,[3] Norio Shimizu[4] and Hiroshi Wakiguchi[7]

[1]*Department of Infectious Diseases, National Research Institute for Child Health and Development, Departments of* [2]*Hematology and* [3]*Developmental Biology and Pediatrics, Graduate School of Medical and Dental Sciences,* [4]*Department of Virology, Division of Medical Science, Medical Research Institute, Tokyo Medical and Dental University, Tokyo,* [5]*Department of Virology, Nagoya University Graduate School of Medicine, Nagoya,* [6]*Department of Internal Medicine/Division of Emerging Infectious Diseases, Tohoku University Graduate School of Medicine, Sendai and* [7]*Department of Pediatrics, Kochi Medical School, Kochi University, Kochi, Japan*

Abstract Epstein–Barr virus (EBV) infection is usually asymptomatic and persists lifelong. Although EBV-infected B cells have the potential for unlimited proliferation, they are effectively removed by the virus-specific cytotoxic T cells, and EBV-associated lymphoproliferative disease develops only in immunocompromised hosts. Rarely, however, individuals without apparent immunodeficiency develop chronic EBV infection with persistent infectious mononucleosis-like symptoms. These patients have high EBV-DNA load in the peripheral blood and systemic clonal expansion of EBV-infected T cells or natural killer (NK) cells. Their prognosis is poor with life-threatening complications including hemophagocytic lymphohistiocytosis, organ failure, and malignant lymphomas. The term "chronic active EBV infection" (CAEBV) is now generally used for this disease. The geographical distribution of CAEBV is markedly uneven and most cases have been reported from Japan and other East Asian countries. Here we summarize the current understanding of CAEBV and describe the recent progress of CAEBV research in Japan.

Key words chronic active EBV infection, EBV-associated hemophagocytic lymphohistiocytosis, EBV-associated T/NK-cell lymphoproliferative disease, Epstein–Barr virus, flow-cytometric *in situ* hybridization, hydroa vacciniforme, hypersensitivity to mosquito bites, mouse model.

Epstein–Barr virus (EBV) was discovered in cultured cells of Burkitt lymphoma as the first human tumor virus.[1] Since then EBV has been found to be associated with a number of malignancies, including Hodgkin lymphoma, nasopharyngeal carcinoma, and gastric carcinoma.[2] Despite this close association with these malignancies, EBV was found to be a ubiquitous virus infecting >90% of the adult population worldwide. EBV-associated malignancies thus develop in a restricted fraction of hosts through collective effects of various factors, including host genetic background and environmental factors, as well as functions of EBV genes. EBV infection in humans is usually asymptomatic and persists lifelong as a latent infection, although primary infection later than adolescence frequently results in infectious mononucleosis (IM). IM is caused by transient proliferation of EBV-infected B cells accompanied by excessive response of EBV-specific cytotoxic T cells (CTL). The main target of EBV is B cells and epithelial cells, and EBV has a unique biological activity to transform B cells and establish immortalized lymphoblastoid cell lines. Given that EBV-transformed cells express at least nine viral proteins including the highly immunogenic EBV nuclear antigen 3 (EBNA3) and EBNA2 (the latency III type EBV gene expression), they are readily removed by the virus-specific CTL and the virus does not cause lymphoproliferative disease (LPD) in normal immunocompetent hosts.[3] In immunocompromised hosts such as transplant recipients and AIDS patients, however, EBV-transformed cells are not efficiently removed and may cause EBV-associated B-cell LPD.

Rare EBV-infected individuals without apparent immunodeficiency present with persistent or recurring IM-like symptoms including fever, hepatosplenomegaly, lymphadenopathy, and liver dysfunction, as well as high EBV-DNA load in the peripheral blood.[4–7] The term "chronic active EBV infection" (CAEBV) is now generally used to describe this disease. Patients with CAEBV encountered in Japan and other East Asian countries have poor prognosis and are characterized by clonal expansion of EBV-infected T cells or natural killer (NK) cells.[8–11] In contrast, a similar disease with less morbidity and mortality has been reported from Western countries and it is usually associated with

Correspondence: Shigeyoshi Fujiwara, MD PhD, Department of Infectious Diseases, National Research Institute for Child Health and Development, 2-10-1 Okura, Setagaya-ku, Tokyo 157-8535, Japan. Email: fujiwara-s@ncchd.go.jp

Received 24 December 2013; accepted 23 January 2014.

proliferation of EBV-infected B cells.[12] In this review, focused on CAEBV as an EBV-associated T/NK-cell LPD (EBV$^+$ T/NK-LPD), we summarize the current understanding of the disease and describe the authors' own recent work subsidized by grants from the Ministry of Health Labour and Welfare of Japan.

Clinical characteristics of CAEBV and other EBV-associated T/NK-LPD

As described in the previous section, IM-like symptoms are the main symptoms of CAEBV.[4–7] Other clinical manifestations include thrombocytopenia, anemia, pancytopenia, diarrhea, and uveitis. Peripheral blood EBV-DNA load regularly exceeds $10^{2.5}$ copies/μg DNA.[13] High-level production of various cytokines, including interleukin (IL)-1β, IL-10, and interferon (IFN)-γ has been detected in CAEBV patients and is thought to play an important role in inflammatory symptoms of the disease.[14–16] CAEBV can be classified into the T-cell and NK-cell types, depending on which lymphocyte subset is mainly infected with EBV. A survey of Japanese CAEBV patients found that the T-cell type is associated with less favorable prognosis than the NK-cell type.[17,18] CAEBV was included in the 2008 World Health Organization (WHO) classification of lymphomas as the systemic EBV$^+$ T-cell LPD of childhood.[19]

Although the clinical course of CAEBV is chronic, patients often develop fatal complications such as multi-organ failure, disseminated intravascular coagulopathy (DIC), digestive tract ulcer/perforation, coronary artery aneurysms, and malignant lymphomas, as well as EBV-associated hemophagocytic lymphohistiocytosis (EBV-HLH).[7] HLH is a hyper-inflammatory condition caused by overproduction of cytokines by excessively activated T cells and macrophages. Clinical characteristics of HLH include fever, hepatosplenomegaly, pancytopenia, hypertriglyceridemia, DIC, and liver dysfunction.[20]EBV-HLH usually occurs following primary EBV infection and is itself characterized by clonal proliferation of EBV-infected T or NK cells (most often CD8$^+$ T cells).[21,22] EBV-HLH can also occur in association with X-linked lymphoproliferative disease (XLP) and XIAP deficiency.[23]

Patients with CAEBV may have characteristic cutaneous complications, namely hypersensitivity to mosquito bites (HMB) and hydroa vacciniforme (HV), that are themselves distinct EBV$^+$ T/NK-LPD characterized by clonal proliferation of EBV-infected T or NK cells. Both HMB and HV can occur independently or in association with CAEBV. HV is a childhood photosensitivity disorder, characterized by necrotic vesiculopapules on sun-exposed areas.[24] EBV-DNA level is elevated in patients' peripheral blood, and histochemical analysis of skin lesions indicates infiltration of T cells expressing EBV-encoded small RNA (EBER).[25]Although most cases of HV resolve by early adulthood, HV overlapping with CAEBV may eventually develop into EBV-positive malignant lymphoma, which was included in the 2008 WHO classification of lymphoma as the hydroa vacciniforme-like lymphoma.[19,26] HMB is characterized by severe local skin reactions to mosquito bites including erythematous swelling with bullae, necrotic ulcerations, and depressed scars.[27] These local reactions may be accompanied by general symptoms such as high fever, lymphadenopathy, and liver dysfunction. Most HMB patients have EBV infection in NK cells in skin lesions and peripheral blood.[28,29] HMB patients without systemic symptoms may eventually develop CAEBV.[28]

Prospective clinicopathologic analysis of CAEBV and other EBV$^+$ T/NK-LPD

Chronic active EBV infection, EBV-HLH, HMB, and HV are thus distinct but overlapping entities categorized as EBV$^+$ T/NK-LPD. The higher incidence of these diseases in East Asian countries and their occasional coincidence in a single patient imply a common pathogenesis.[7,30] Kimura *et al.* performed a large-scale prospective study of Japanese EBV$^+$ T/NK-LPD.[31] A total of 108 cases of EBV$^+$ T/NK-LPD (80 cases of CAEBV, 15 cases of EBV-HLH, nine cases of HMB, and four cases of HV) were analyzed. They found that the clinical profile of EBV$^+$ T/NK-LPD is closely linked with the lineage of EBV-infected cells. More than half (53%) of EBV-HLH patients had EBV in the CD8$^+$ T-cell subset, in contrast to the low incidence of EBV infection in this subset in the other EBV$^+$ T/NK-LPD. Most HMB patients (89%) had EBV-infected NK cells, whereas the majority (75%) of HV patients had EBV-infected γδT cells. In a median follow-up period of 46 months, 47 patients (44%) died of severe organ complications and 13 (12%) developed overt lymphoma or leukemia. Age of onset ≥8 years and liver dysfunction were risk factors for mortality, and transplant patients had better prognosis. Patients with CD4$^+$ T-cell infection had shorter survival as compared with those with NK-cell infection. Because shorter time from onset to hematopoietic stem cell transplantation (HSCT) and inactive disease at HSCT were associated with longer survival, earlier HSCT in good condition was considered preferable. Among the 108 patients enrolled, four patients developed aggressive NK-cell leukemia (ANKL) and six patients developed extranodal NK/T-cell lymphoma (ENKL). It is thus conceivable that a certain fraction of patients with ANKL and ENKL developed these malignancies as a consequence of CAEBV.[32,33]

Characteristics of adult CAEBV

Chronic active EBV infection has been described mainly as a disease of childhood and young adulthood; the mean age of onset was estimated to be 11.3 years.[18] Recently, however, an increasing number of adult patients fulfilling the criteria of CAEBV has been reported. This may be a true increase in the incidence of adult-onset CAEBV or reflect improved recognition of this disease by physicians. Arai *et al.* reviewed 23 cases of adult-onset CAEBV and described the characteristics.[34] In 87% of adult cases, T cells were infected with EBV, whereas in childhood-onset cases, the T- and NK-cell types were equally frequent. Adult-onset cases appeared rapidly progressive and more aggressive, although the number of patients analyzed was limited. Further investigation with a larger number of patients is required to elucidate the characteristics of adulthood CAEBV and its relation to the childhood counterpart.

Recurrence of CAEBV with EBV-infected, donor-derived T cells following HSCT

The relative prevalence of CAEBV in East Asia and in natives of Central and South America implies a genetic background for its pathogenesis. Recently HLA-A*26, a major histocompatibility complex class I allele relatively common in East Asia, was found to be associated with an increased risk for EBV$^+$ T/NK-LPD.[35] Although the possible involvement of EBV strains with increased propensity to induce T/NK-cell lymphoproliferation cannot be formally denied, it is highly unlikely because outbreaks and familial transmission of CAEBV have not been reported. Arai *et al.* reported an intriguing case of CAEBV in which the patient experienced relapse after bone marrow transplantation.[36] A 35-year-old female patient with CAEBV of the CD8 type had HSCT from an unrelated male donor following myeloablative preconditioning with total body irradiation. The serologic HLA types of the patient and the donor were identical, whereas the DNA types were different in two HLA-DR alleles. Although the peripheral blood EBV-DNA was undetectable at 1 month after HSCT and remained so for nearly 12 months, the patient's EBV-DNA load increased again and reached 1.0×10^5 copies/μg DNA. EBV was found primarily in CD8$^+$ T cells again, but the EBV-infected cells now had an XY karyotype, clearly indicating their donor origin. Sequencing analysis of the variable region of the EBV-encoded *LMP1* gene showed that the virus strain infecting the CD8$^+$ T cells was different before and after bone marrow transplantation, suggesting that the repeated episodes of CAEBV were not caused by a rare EBV strain with an unusual biological activity. If we do not suppose that these two consecutive episodes of CAEBV in a single patient occurred only by chance, these findings suggest that the patient may have had a certain genetic background that exerts its direct effects on cellular lineages unrelated to hematopoietic stem cells.

Pathophysiology of CAEBV

The pathogenesis of CAEBV is not understood. Most T and NK cells do not express the EBV receptor CD21, and the mechanism of their infection with EBV is not clear. Transfer of CD21 from B cells to NK cells through immunological synapse may render the latter cells accessible to EBV.[37] The mechanism by which EBV induces proliferation of T and NK cells is not known either. EBV-induced expression of CD40 and its engagement by CD40L may have a role in the survival of EBV-infected T and NK cells of CAEBV patients.[38] Given that EBV-positive T or NK cells have been occasionally found in the tonsil and peripheral blood of IM patients, ectopic EBV infection in T or NK cells does not necessarily lead to the development of CAEBV.[39–41] Although EBV-infected T and NK cells in CAEBV patients and cell lines derived from them do not express the most immunodominant EBNA3 and EBNA2, they express EBNA1, latent membrane protein 1 (LMP1) and LMP2 (the latency II type EBV gene expression) that are frequently recognized by EBV-specific CTL.[3,42–45] Hosts with normal immune functions are thus expected to have the capacity to recognize EBV-infected T and NK cells. It is thus conceivable that patients with CAEBV have a certain defect in immunologic functions that causes inefficient recognition and/or killing of EBV-infected latency II cells. Indeed, deficiency in cellular immune responses to EBV has been detected in patients with CAEBV.[46–48]The defect in T-cell responses to LMP2A might be particularly relevant to this issue.[47] Interestingly, a patient with clinical manifestations similar to CAEBV, although the virus was found in his B cells, was found to have mutations in the gene encoding perforin, which has a critical role in granule-mediated killing of target cells.[49] None of the other patients with CAEBV, however, were found to have a mutation in the *perforin* gene. Mutations of the genes responsible for XLP, XIAP deficiency, and familial HLH (except for the type 2 that is caused by mutations of *perforin*) have not been reported for patients with CAEBV.[7]

Clonal proliferation of EBV-infected T or NK cells in CAEBV and other EBV$^+$ T/NK-LPD implies that these diseases have a malignant nature. CAEBV, however, is a chronic disease and patients with clonal expansion of EBV-infected T or NK cells may remain in a stable condition for years without treatment.[18] Overt malignant lymphoma occurs usually after a long course of disease. Therefore CAEBV may represent, at least in its early phase, a premalignant or smoldering phase of EBV-positive leukemia/lymphomas. Ohshima *et al.* proposed a pathological categorization of CAEBV into a continuous spectrum ranging from a smoldering phase to overt leukemia/lymphoma.[50] Clonality of EBV-infected T or NK cells in CAEBV may not necessarily indicate a malignant phenotype; acquisition of clonality might be a result of other selective processes such as immune escape.

Mouse xenograft models for EBV$^+$ T/NK-LPD

Animal models for EBV$^+$ T/NK-LPD have not been available, rendering research on their pathogenesis and therapy difficult. Imadome *et al.* transplanted peripheral blood mononuclear cells (PBMC) isolated from patients with CAEBV and EBV-HLH into immunodeficient mice of the NOD/Shi-*scid*/IL-2Rγ^{null} (NOG) strain, and successfully reproduced major features of these diseases including systemic monoclonal proliferation of EBV-infected T or NK cells and hypercytokinemia (Fig. 1).[51] Although many features were common to CAEBV and EBV-HLH model mice, hemorrhagic lesions in the abdominal and thoracic cavities and extreme hypercytokinemia were unique to the latter model, indicating that these mouse models reflect the differences in the pathophysiology of the original diseases. Importantly, these models revealed an essential role of CD4$^+$ T cells in the engraftment of EBV-infected T and NK cells. *In vivo* depletion of CD4$^+$ T cells following transplantation effectively prevented the engraftment of EBV-infected cells of not only the CD4$^+$ lineage but also the CD8$^+$ and CD56$^+$ lineages. Furthermore, OKT-4 antibody given after engraftment was also effective to reduce EBV-DNA load in the peripheral blood and major organs (Imadome *et al.*, unpubl. data 2012). These results suggest that therapeutic approaches targeting CD4$^+$ T cells may be possible.

Diagnosis and monitoring of CAEBV

Prolonged or relapsing symptoms of IM are the major clue to the diagnosis of CAEBV. Although elevated serum antibody titers

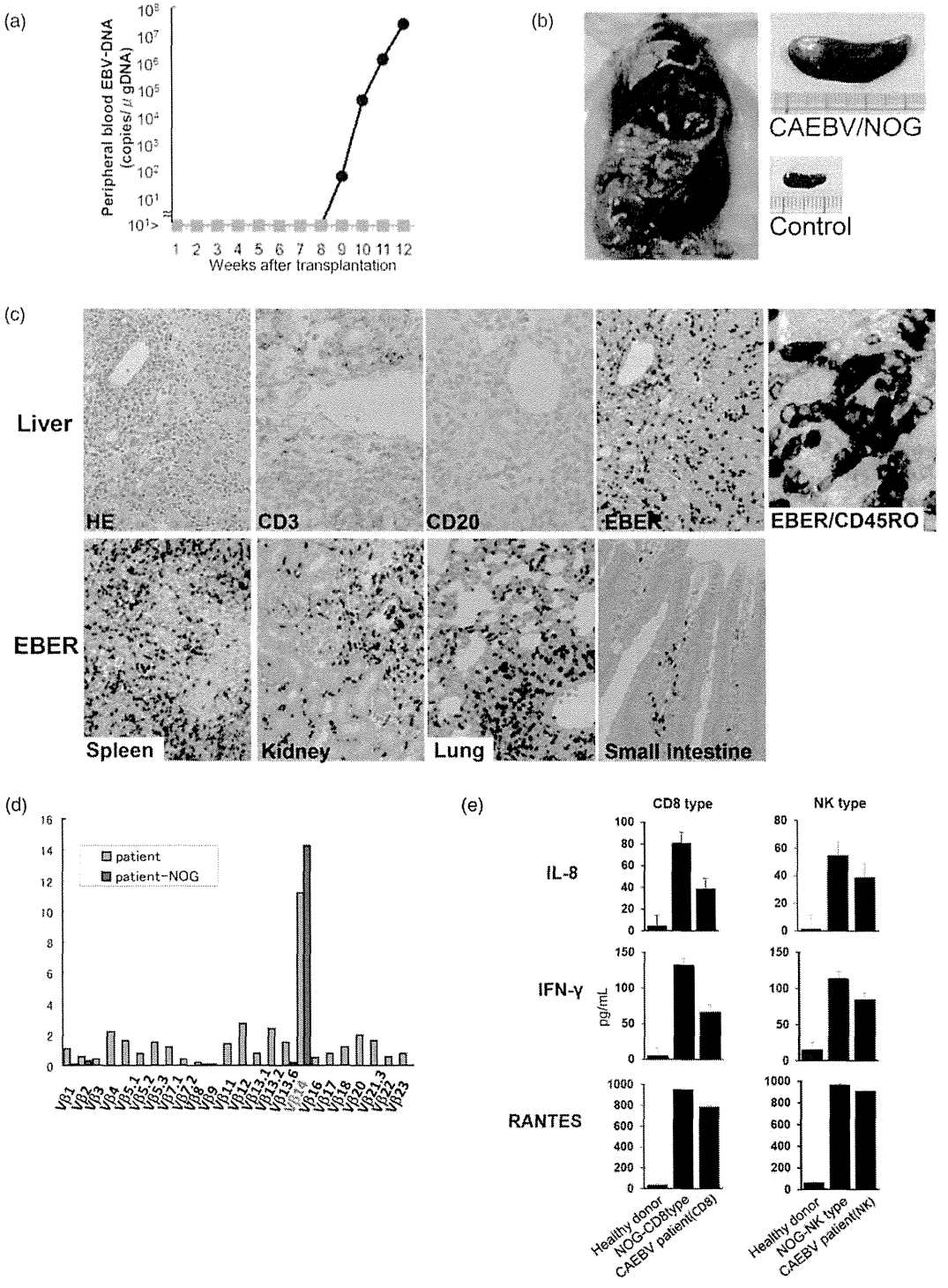

Fig. 1 Mouse xenograft model of chronic active Epstein–Barr virus infection (CAEBV). Peripheral blood mononuclear cells (PBMC) of a patient with the CD8 type CAEBV were transplanted i.v. into NOD/Shi-*scid Il2rg* ^{null} (NOG) mice. (a) Measurement of peripheral blood EBV-DNA. EBV-DNA load increased rapidly from approximately 9 weeks after transplantation, when (●) whole PBMC but not (□) isolated $CD8^+$ cells were transplanted. (b) Splenomegaly of a model mouse. (c) Pathological analysis. Histochemical analysis showed massive infiltration of EBV-encoded small RNA $(EBER)^+/CD20^-/CD3^+/CD45RO^+$ cells in most major organs including the spleen, kidneys, lungs, and small intestine. (d) T-cell receptor (TCR) repertoire analysis of peripheral blood T cells isolated from the patient and a mouse that received the patient's PBMC. An identical clone of EBV-infected T cells expressing Vβ14 is proliferating in the patient and the corresponding mouse. (e) Human cytokine levels in CAEBV model mice. Serum levels of interleukin (IL)-8, interferon (IFN)-γ, and regulated on activation, normal T-cell expressed and secreted (RANTES) were measured in mice that were transplanted with PBMC isolated from either a CD8-type or an NK-type CAEBV patient. The same set of cytokines was also quantified in the sera of the original patients and healthy donors. Modified from *PLoS Pathog.* 2011; **7**(10): e1002326.[51]

against EBV-encoded antigens are often found, this does not always occur, and normal titers of anti-EBV antibodies should not preclude the diagnosis of CAEBV.[7] Diagnostic criteria for CAEBV have been published.[13] Quantification of peripheral blood EBV-DNA is most important for diagnosis and a finding of elevation should be followed by identification of EBV-infected T or NK cells. Quantification of EBV-DNA is, however, influenced by many factors and the results can vary in different laboratories.[52] Recently, therefore, an international standard EBV-DNA sample for normalization became available from the National Institute for Biological Standards and Controls, USA. Given that CAEBV is a chronic disease that may progress to overt malignancy and early HSCT in a better clinical condition is recommended, precise monitoring of patient clinical parameters is particularly important.

Flow-cytometric in situ *hybridization for identification of EBV-infected cells*

Diagnosis of CAEBV requires exact phenotyping of EBV-infected cells. This has usually been done with immunobead sorting of PBMC into lymphocyte subsets, followed by measurement of EBV-DNA in each subset using quantitative polymerase chain reaction. These processes are, however, time-consuming and require specific skills. Kimura *et al.* developed a new method termed "flow-cytometric *in situ* hybridization" (FISH) to phenotype EBV-infected cells (Fig. 2).[53,54] They utilized a fluorescence-labeled peptide nucleic acid (PNA) probe complementary to EBER and succeeded in detecting EBER on flow cytometry. Following reaction with antibodies specific to surface markers, PBMC were permeabilized and subjected to *in situ* hybridization with the PNA probe. EBER probes and surface-bound antibodies were then detected simultaneously on flow cytometry. EBV-infected cells with a certain phenotype can be directly counted using FISH, which is less laborious than the current method. They showed that FISH can be applied for the diagnosis of EBV^+ T/NK-LPD, and that EBV infects mainly γδT cells in HV.[53–55]

MicroRNA as a potential biomarker of CAEBV

MicroRNA (miRNA) is a small non-coding RNA of 18–25 nucleotides that plays a critical role in the regulation of cellular proliferation, differentiation, and apoptosis through negatively regulating mRNA translation.[56] miRNAs are encoded not only by cells but also by viruses; EBV is actually the first virus shown to encode miRNAs.[57] Two clusters of EBV-encoded miRNAs have been identified: miR–*Bam*HI fragment H rightward open reading frame 1 (miR-BHRF1) and miR–*Bam* HI A region rightward transcripts (miR-BART).[58] Kawano *et al.* reported that plasma levels of miR-BART 1-5p, 2-5p, 5, and 22 are significantly higher in patients with CAEBV than in those with IM and healthy controls.[59] Plasma miR-BART 2-5p, 4, 7, 13, 15, and 22 levels were significantly elevated in CAEBV patients with active disease compared to those with inactive disease. miR-BART 13 level could differentiate patients with active disease from those with inactive disease, with a clear cut-off. Similarly, plasma miR-BART 2-5p and 15 levels could clearly differentiate patients with complete remission from others. Importantly, plasma EBV-DNA level did not show any significant correlation with these clinical parameters. These results suggest that EBV-encoded miRNA in plasma may be a useful biomarker for the diagnosis and monitoring of CAEBV.

Therapy of CAEBV

Various therapies have been tried for the treatment of CAEBV, including antiviral, chemotherapeutic, and immunomodulatory drugs, with only limited success. These regimens induced sustained complete remission in only exceptional cases and HSCT is at present the only curative therapy for CAEBV.[60] The current event-free survival rate for CAEBV patients following HSCT is estimated to be 0.561 ± 0.086.[61]Very recently, Kawa *et al.* reported excellent results of HSCT following non-destructive pretreatment (reduced intensity hematopoietic stem cell transplantation; RIST).[62] For 18 pediatric patients with CAEBV who were treated with RIST, 3 year event-free survival was $85.0 \pm 8.0\%$ and the 3 year overall survival rate was $95.0 \pm 4.9\%$. HSCT is thus the therapy of choice for CAEBV, but HSCT is still accompanied by substantial risk and CAEBV patients have high risk for transplantation-related complications.[18] It is therefore desirable to develop novel therapies that do not depend on HSCT. Preclinical studies of two candidate drugs for CAEBV have been carried out recently and gave hopeful results.

Bortezomib, known as an inhibitor of 26S proteasome,[63] also has an inhibitory effect on the cellular transcription factor NF-κB. Because the survival and proliferation of EBV-transformed B cells are critically dependent on NF-κB activity, bortezomib has been shown to induce apoptosis in these cells.[64] Iwata *et al.* investigated the effect of bortezomib on EBV-infected T-cell lines including those derived from CAEBV.[65] Bortezomib induced apoptosis in all human T-cell lymphoma cell lines examined, whether or not they were infected with EBV. In addition, bortezomib induced the expression of EBV lytic-cycle genes *BZLF1* and *gp350/220*, as has been reported for EBV-infected B-cell lines.[66] Bortezomib also induced apoptosis specifically in EBV-infected T or NK cells cultured *ex vivo* from patients with EBV^+T/NK-LPD.

Valproic acid is a widely used anti-epileptic drug and is also known as a potent histone deacetylase (HDAC) inhibitor. HDAC inhibitors have potent anticancer activities with proven efficacy in various human malignancies. Valproic acid induces lytic infection in EBV-infected B-lymphoblastoid and gastric carcinoma cell lines and thereby potentiates the effects of chemotherapeutic agents both *in vitro* and *in vivo*.[67] Iwata *et al.* examined the effect of valproic acid on EBV-infected T and NK cell lines.[68] They found that this agent induces apoptosis in human EBV-infected T and NK cells. Use of the drug with the NF-κB inhibitor bortezomib had an additive effect. In contrast to the previous results with EBV-infected B-cell lines, valproic acid did not induce lytic infection in the virus-infected T- and NK-cell lines, indicating that the apoptosis-inducing effect of valproic acid is not dependent on induction of EBV lytic cycle.

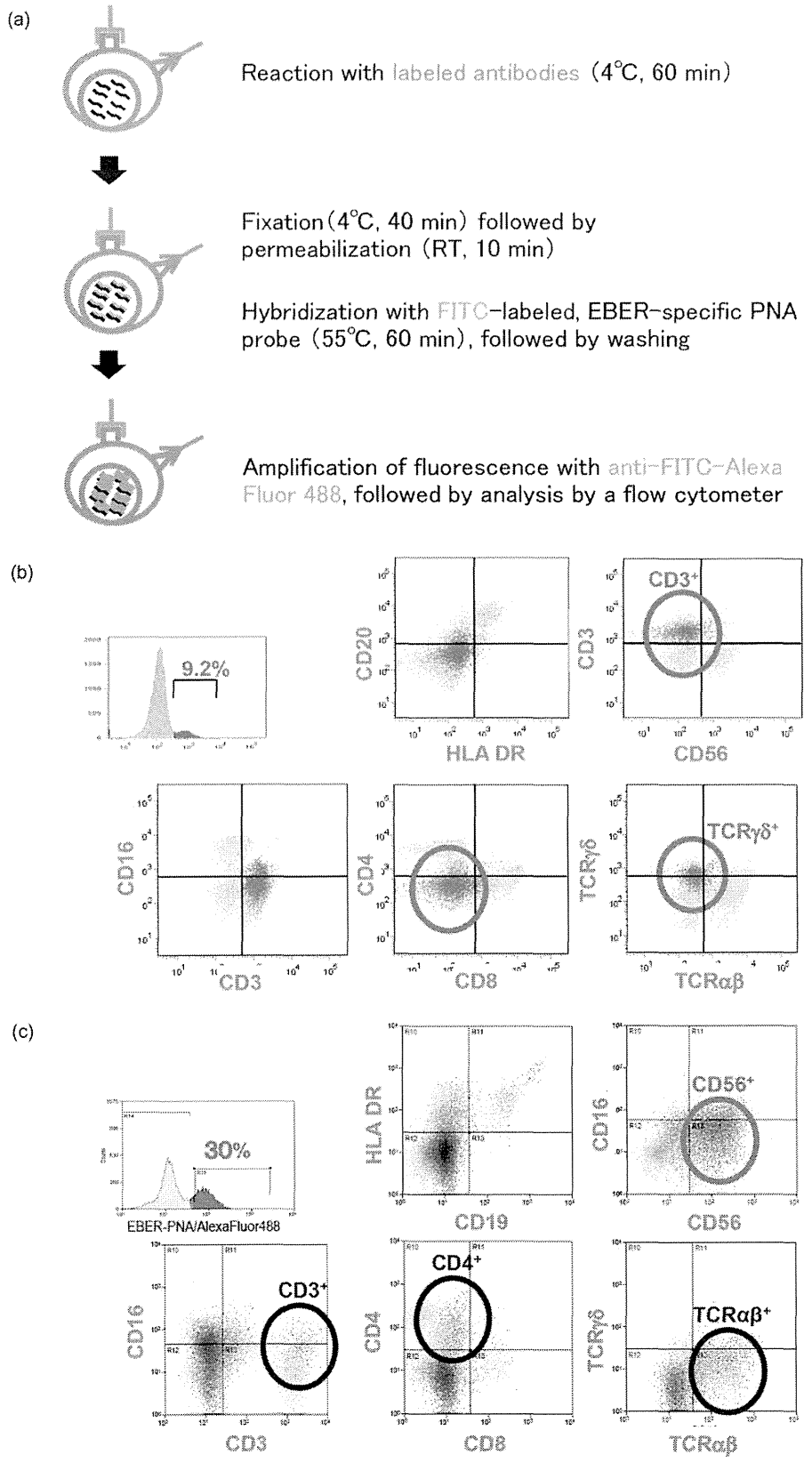

Fig. 2 Flow-cytometric *in situ* hybridization (FISH). (a) Protocol of FISH. (b) Results of FISH in a patient with hydroa vacciniforme. Red, EBER-positive cells; blue, EBER-negative cells. Most EBV-infected cells in the peripheral blood of this patient had the phenotype $CD3^+/CD4^-/CD8^-/TCR\gamma\delta^+$. (c) Results of FISH in a patient with the NK-cell type chronic active Epstein–Barr virus infection. Red, EBER-positive cells; blue, EBER-negative cells. The majority of EBV-infected cells in the peripheral blood of this patient were $CD56^+$ NK cells. Also, a small proportion of $TCR\alpha\beta^+/CD3^+/CD4^+$ cells also contained EBV. EBER, Epstein–Barr virus-encoded small RNA; FITC, fluorescein isothiocyanate; PNA, peptide nucleic acid; RT, reverse transcription.

Perspective

Significant progress has been made in the research of many aspects of CAEBV, including pathophysiology, diagnosis, monitoring, and therapy, but the fundamental cause of the disease has not been elucidated. The recent development of novel technologies for genetic analysis, including new-generation sequencing, may enable identification of genetic alterations responsible for CAEBV. Given that CAEBV is an uncommon disease, it may sometimes take years for the correct diagnosis to be reached. The advanced techniques required for this also make the diagnosis of CAEBV difficult. Although there is a consensus that early HSCT produces a better result, the decision to have HSCT is often difficult, especially when the patient is in a stable condition without severe symptoms. Establishing a standard clinical guideline for the diagnosis and treatment of CAEBV will alleviate these problems and facilitate quick and accurate diagnosis, followed by timely intervention with the right choice of treatment.

Acknowledgments

The authors' works described in this article have been funded by grants from the Ministry of Health Labour and Welfare of Japan for the Research on Measures for Intractable Diseases (H21-Nanchi-094, H22-Nanchi-080, H24-Nanchi-046).

References

1 Epstein MA, Achong BG, Barr YM. Virus particles in cultured lymphoblasts from Burkitt's lymphoma. *Lancet* 1964; **1**: 702–3.
2 Longnecker RM, Kieff E, Cohen JI. Epstein-Barr virus. In: Knipe DM, Howley PM (eds). *Fields Virology*, Vol. **2**, 6th edn. Lippincott Williams and Wilkins, Philadelphia, PA, 2013; 1898–959.
3 Hislop AD, Taylor GS, Sauce D, Rickinson AB. Cellular responses to viral infection in humans: Lessons from Epstein-Barr virus. *Annu. Rev. Immunol.* 2007; **25**: 587–617.
4 Rickinson AB. Chronic, symptomatic Epstein-Barr virus infection. *Immunol. Today* 1986; **7**: 13–14.
5 Straus SE. The chronic mononucleosis syndrome. *J. Infect. Dis.* 1988; **157**: 405–12.
6 Okano M. Overview and problematic standpoints of severe chronic active Epstein-Barr virus infection syndrome. *Crit. Rev. Oncol. Hematol.* 2002; **44**: 273–82.
7 Kimura H. Pathogenesis of chronic active Epstein-Barr virus infection: Is this an infectious disease, lymphoproliferative disorder, or immunodeficiency? *Rev. Med. Virol.* 2006; **16**: 251–61.
8 Kikuta H, Taguchi Y, Tomizawa K *et al.* Epstein-Barr virus genome-positive T lymphocytes in a boy with chronic active EBV infection associated with Kawasaki-like disease. *Nature* 1988; **333**: 455–7.
9 Jones JF, Shurin S, Abramowsky C *et al.* T-cell lymphomas containing Epstein-Barr viral DNA in patients with chronic Epstein-Barr virus infections. *N. Engl. J. Med.* 1988; **318**: 733–41.
10 Ishihara S, Tawa A, Yumura-Yagi K *et al.* Clonal T-cell lymphoproliferation containing Epstein-Barr (EB) virus DNA in a patient with chronic active EB virus infection. *Jpn J. Cancer Res.* 1989; **80**: 99–101.
11 Kawa-Ha K, Ishihara S, Ninomiya T *et al.* CD3-negative lymphoproliferative disease of granular lymphocytes containing Epstein-Barr viral DNA. *J. Clin. Invest.* 1989; **84**: 51–5.
12 Cohen JI, Jaffe ES, Dale JK *et al.* Characterization and treatment of chronic active Epstein-Barr virus disease: A 28-year experience in the United States. *Blood* 2011; **117**: 5835–49.
13 Okano M, Kawa K, Kimura H *et al.* Proposed guidelines for diagnosing chronic active Epstein-Barr virus infection. *Am. J. Hematol.* 2005; **80**: 64–9.
14 Lay JD, Tsao CJ, Chen JY, Kadin ME, Su IJ. Upregulation of tumor necrosis factor-alpha gene by Epstein-Barr virus and activation of macrophages in Epstein-Barr virus-infected T cells in the pathogenesis of hemophagocytic syndrome. *J. Clin. Invest.* 1997; **100**: 1969–79.
15 Xu J, Ahmad A, Jones JF *et al.* Elevated serum transforming growth factor beta1 levels in Epstein-Barr virus-associated diseases and their correlation with virus-specific immunoglobulin A (IgA) and IgM. *J. Virol.* 2000; **74**: 2443–6.
16 Ohga S, Nomura A, Takada H *et al.* Epstein-Barr virus (EBV) load and cytokine gene expression in activated T cells of chronic active EBV infection. *J. Infect. Dis.* 2001; **183**: 1–7.
17 Kimura H, Hoshino Y, Kanegane H *et al.* Clinical and virologic characteristics of chronic active Epstein-Barr virus infection. *Blood* 2001; **98**: 280–86.
18 Kimura H, Morishima T, Kanegane H *et al.* Prognostic factors for chronic active Epstein-Barr virus infection. *J. Infect. Dis.* 2003; **187**: 527–33.
19 Jaffe ES. The 2008 WHO classification of lymphomas: Implications for clinical practice and translational research. *Hematology Am. Soc. Hematol. Educ. Program* 2009; 523–31.
20 Henter JI, Horne A, Arico M *et al.* HLH-2004: Diagnostic and therapeutic guidelines for hemophagocytic lymphohistiocytosis. *Pediatr. Blood Cancer* 2007; **48**: 124–31.
21 Kikuta H, Sakiyama Y, Matsumoto S *et al.* Fatal Epstein-Barr virus-associated hemophagocytic syndrome. *Blood* 1993; **82**: 3259–64.
22 Kawaguchi H, Miyashita T, Herbst H *et al.* Epstein-Barr virus-infected T lymphocytes in Epstein-Barr virus-associated hemophagocytic syndrome. *J. Clin. Invest.* 1993; **92**: 1444–50.
23 Yang X, Miyawaki T, Kanegane H. SAP and XIAP deficiency in hemophagocytic lymphohistiocytosis. *Pediatr. Int.* 2012; **54**: 447–54.
24 Goldgeier MH, Nordlund JJ, Lucky AW, Sibrack LA, McCarthy MJ, McGuire J. Hydroa vacciniforme: Diagnosis and therapy. *Arch. Dermatol.* 1982; **118**: 588–91.
25 Iwatsuki K, Xu Z, Takata M *et al.* The association of latent Epstein-Barr virus infection with hydroa vacciniforme. *Br. J. Dermatol.* 1999; **140**: 715–21.
26 Iwatsuki K, Ohtsuka M, Akiba H, Kaneko F. Atypical hydroa vacciniforme in childhood: From a smoldering stage to Epstein-Barr virus-associated lymphoid malignancy. *J. Am. Acad. Dermatol.* 1999; **40**: 283–4.
27 Ishihara S, Ohshima K, Tokura Y *et al.* Hypersensitivity to mosquito bites conceals clonal lymphoproliferation of Epstein-Barr viral DNA-positive natural killer cells. *Jpn J. Cancer Res.* 1997; **88**: 82–7.
28 Kawa K, Okamura T, Yagi K, Takeuchi M, Nakayama M, Inoue M. Mosquito allergy and Epstein-Barr virus-associated T/natural killer-cell lymphoproliferative disease. *Blood* 2001; **98**: 3173–4.
29 Ishihara S, Okada S, Wakiguchi H, Kurashige T, Hirai K, Kawa-Ha K. Clonal lymphoproliferation following chronic active Epstein-Barr virus infection and hypersensitivity to mosquito bites. *Am. J. Hematol.* 1997; **54**: 276–81.
30 Iwatsuki K, Yamamoto T, Tsuji K *et al.* A spectrum of clinical manifestations caused by host immune responses against Epstein-Barr virus infections. *Acta Med. Okayama* 2004; **58**: 169–80.
31 Kimura H, Ito Y, Kawabe S *et al.* EBV-associated T/NK-cell lymphoproliferative diseases in nonimmunocompromised hosts: Prospective analysis of 108 cases. *Blood* 2012; **119**: 673–86.
32 Isobe Y, Aritaka N, Setoguchi Y *et al.* T/NK cell type chronic active Epstein-Barr virus disease in adults: An underlying condition for Epstein-Barr virus-associated T/NK-cell lymphoma. *J. Clin. Pathol.* 2012; **65**: 278–82.

33 Takahashi E, Ohshima K, Kimura H *et al.* Clinicopathological analysis of the age-related differences in patients with Epstein-Barr virus (EBV)-associated extranasal natural killer (NK)/T-cell lymphoma with reference to the relationship with aggressive NK cell leukaemia and chronic active EBV infection-associated lymphoproliferative disorders. *Histopathology* 2011; **59**: 660–71.
34 Arai A, Imadome K, Watanabe Y *et al.* Clinical features of adult-onset chronic active Epstein-Barr virus infection: A retrospective analysis. *Int. J. Hematol.* 2011; **93**: 602–9.
35 Ito Y Sr, Torii Y, Kawa K, Kikuta A, Kojima S, Kimura H. HLA-A*26 and HLA-B*52 are associated with a risk of developing EBV-associated T/NK lymphoproliferative disease. *Blood* 2013; ID: bloodjournal_el; 8085.
36 Arai A, Imadome K, Wang L *et al.* Recurrence of chronic active Epstein-Barr virus infection from donor cells after achieving complete response through allogeneic bone marrow transplantation. *Intern. Med.* 2012; **51**: 777–82.
37 Tabiasco J, Vercellone A, Meggetto F, Hudrisier D, Brousset P, Fournie JJ. Acquisition of viral receptor by NK cells through immunological synapse. *J. Immunol.* 2003; **170**: 5993–8.
38 Imadome K, Shimizu N, Arai A *et al.* Coexpression of CD40 and CD40 ligand in Epstein-Barr virus-infected T and NK cells and their role in cell survival. *J. Infect. Dis.* 2005; **192**: 1340–48.
39 Anagnostopoulos I, Hummel M, Kreschel C, Stein H. Morphology, immunophenotype, and distribution of latently and/or productively Epstein-Barr virus-infected cells in acute infectious mononucleosis: Implications for the interindividual infection route of Epstein-Barr virus. *Blood* 1995; **85**: 744–50.
40 Hudnall SD, Ge Y, Wei L, Yang NP, Wang HQ, Chen T. Distribution and phenotype of Epstein-Barr virus-infected cells in human pharyngeal tonsils. *Mod. Pathol.* 2005; **18**: 519–27.
41 Kasahara Y, Yachie A, Takei K *et al.* Differential cellular targets of Epstein-Barr virus (EBV) infection between acute EBV-associated hemophagocytic lymphohistiocytosis and chronic active EBV infection. *Blood* 2001; **98**: 1882–8.
42 Imai S, Sugiura M, Oikawa O *et al.* Epstein-Barr virus (EBV)-carrying and -expressing T-cell lines established from severe chronic active EBV infection. *Blood* 1996; **87**: 1446–57.
43 Yoshioka M, Ishiguro N, Ishiko H, Ma X, Kikuta H, Kobayashi K. Heterogeneous, restricted patterns of Epstein-Barr virus (EBV) latent gene expression in patients with chronic active EBV infection. *J. Gen. Virol.* 2001; **82**: 2385–92.
44 Kimura H, Hoshino Y, Hara S *et al.* Differences between T cell-type and natural killer cell-type chronic active Epstein-Barr virus infection. *J. Infect. Dis.* 2005; **191**: 531–9.
45 Demachi A, Nagata H, Morio T *et al.* Characterization of Epstein-Barr virus (EBV)-positive NK cells isolated from hydroa vacciniforme-like eruptions. *Microbiol. Immunol.* 2003; **47**: 543–52.
46 Tsuge I, Morishima T, Kimura H, Kuzushima K, Matsuoka H. Impaired cytotoxic T lymphocyte response to Epstein-Barr virus-infected NK cells in patients with severe chronic active EBV infection. *J. Med. Virol.* 2001; **64**: 141–8.
47 Sugaya N, Kimura H, Hara S *et al.* Quantitative analysis of Epstein-Barr virus (EBV)-specific CD8+ T cells in patients with chronic active EBV infection. *J. Infect. Dis.* 2004; **190**: 985–8.
48 Fujieda M, Wakiguchi H, Hisakawa H, Kubota H, Kurashige T. Defective activity of Epstein-Barr virus (EBV) specific cytotoxic T lymphocytes in children with chronic active EBV infection and in their parents. *Acta Paediatr. Jpn* 1993; **35**: 394–9.
49 Katano H, Ali MA, Patera AC *et al.* Chronic active Epstein-Barr virus infection associated with mutations in perforin that impair its maturation. *Blood* 2004; **103**: 1244–52.
50 Ohshima K, Kimura H, Yoshino T *et al.* Proposed categorization of pathological states of EBV-associated T/natural killer-cell lymphoproliferative disorder (LPD) in children and young adults: Overlap with chronic active EBV infection and infantile fulminant EBV T-LPD. *Pathol. Int.* 2008; **58**: 209–17.
51 Imadome K, Yajima M, Arai A *et al.* Novel mouse xenograft models reveal a critical role of CD4+ T cells in the proliferation of EBV-infected T and NK cells. *PLoS Pathog.* 2011; **7**: e1002326.
52 Ito Y, Takakura S, Ichiyama S *et al.* Multicenter evaluation of prototype real-time PCR assays for Epstein-Barr virus and cytomegalovirus DNA in whole blood samples from transplant recipients. *Microbiol. Immunol.* 2010; **54**: 516–22.
53 Kimura H, Miyake K, Yamauchi Y *et al.* Identification of Epstein-Barr virus (EBV)-infected lymphocyte subtypes by flow cytometric in situ hybridization in EBV-associated lymphoproliferative diseases. *J. Infect. Dis.* 2009; **200**: 1078–87.
54 Kawabe S, Ito Y, Gotoh K *et al.* Application of flow cytometric in situ hybridization assay to Epstein-Barr virus-associated T/natural killer cell lymphoproliferative diseases. *Cancer Sci.* 2012; **103**: 1481–8.
55 Hirai Y, Yamamoto T, Kimura H *et al.* Hydroa vacciniforme is associated with increased numbers of Epstein-Barr virus-infected gammadeltaT cells. *J. Invest. Dermatol.* 2012; **132**: 1401–8.
56 Bartel DP. MicroRNAs: Target recognition and regulatory functions. *Cell* 2009; **136**: 215–33.
57 Pfeffer S, Zavolan M, Grasser FA *et al.* Identification of virus-encoded microRNAs. *Science* 2004; **304**: 734–6.
58 Cai X, Schafer A, Lu S *et al.* Epstein-Barr virus microRNAs are evolutionarily conserved and differentially expressed. *PLoS Pathog.* 2006; **2**: e23.
59 Kawano Y, Iwata S, Kawada J *et al.* Plasma viral microRNA profiles reveal potential biomarkers for chronic active Epstein-Barr virus infection. *J. Infect. Dis.* 2013; **208**: 771–9.
60 Okamura T, Hatsukawa Y, Arai H, Inoue M, Kawa K. Blood stem-cell transplantation for chronic active Epstein-Barr virus with lymphoproliferation. *Lancet* 2000; **356**: 223–4.
61 Sato E, Ohga S, Kuroda H *et al.* Allogeneic hematopoietic stem cell transplantation for Epstein-Barr virus-associated T/natural killer-cell lymphoproliferative disease in Japan. *Am. J. Hematol.* 2008; **83**: 721–7.
62 Kawa K, Sawada A, Sato M *et al.* Excellent outcome of allogeneic hematopoietic SCT with reduced-intensity conditioning for the treatment of chronic active EBV infection. *Bone Marrow Transplant.* 2011; **46**: 77–83.
63 Adams J. Proteasome inhibition: A novel approach to cancer therapy. *Trends Mol. Med.* 2002; **8**: S49–54.
64 Zou P, Kawada J, Pesnicak L, Cohen JI. Bortezomib induces apoptosis of Epstein-Barr virus (EBV)-transformed B cells and prolongs survival of mice inoculated with EBV-transformed B cells. *J. Virol.* 2007; **81**: 10029–36.
65 Iwata S, Yano S, Ito Y *et al.* Bortezomib induces apoptosis in T lymphoma cells and natural killer lymphoma cells independent of Epstein-Barr virus infection. *Int. J. Cancer* 2011; **129**: 2263–73.
66 Fu DX, Tanhehco YC, Chen J *et al.* Virus-associated tumor imaging by induction of viral gene expression. *Clin. Cancer Res.* 2007; **13**: 1453–8.
67 Feng WH, Kenney SC. Valproic acid enhances the efficacy of chemotherapy in EBV-positive tumors by increasing lytic viral gene expression. *Cancer Res.* 2006; **66**: 8762–9.
68 Iwata S, Saito T, Ito Y *et al.* Antitumor activities of valproic acid on Epstein-Barr virus-associated T and natural killer lymphoma cells. *Cancer Sci.* 2012; **103**: 375–81.

Molecular and Virological Evidence of Viral Activation From Chromosomally Integrated Human Herpesvirus 6A in a Patient With X-Linked Severe Combined Immunodeficiency

Akifumi Endo,[1,2] Ken Watanabe,[3] Tamae Ohye,[4] Kyoko Suzuki,[5] Tomoyo Matsubara,[5] Norio Shimizu,[3] Hiroki Kurahashi,[4] Tetsushi Yoshikawa,[6] Harutaka Katano,[7] Naoki Inoue,[8] Kohsuke Imai,[1] Masatoshi Takagi,[1] Tomohiro Morio,[1] and Shuki Mizutani[1]

[1]Department of Pediatrics and Developmental Biology, Tokyo Medical and Dental University, [2]Department of Pediatrics, Tokyo Metropolitan Cancer and Infectious Diseases Center, Komagome Hospital, and [3]Department of Virology, Tokyo Medical and Dental University, [4]Division of Molecular Genetics, Fujita Health University, Toyoake; [5]Department of Pediatrics, Juntendo University Urayasu Hospital, [6]Department of Pediatrics, Fujita Health University, Toyoake, Departments of [7]Pathology and [8]Virology I, National Institute of Infectious Diseases, Tokyo, Japan

(See the Editorial Commentary by Flamand on pages 549–51.)

It has been unclear whether chromosomally integrated human herpesvirus 6 (ciHHV-6) can be activated with pathogenic effects on the human body. We present molecular and virological evidence of ciHHV-6A activation in a patient with X-linked severe combined immunodeficiency. These findings have significant implications for the management of patients with ciHHV-6.

Keywords. ciHHV-6; HHV-6; X-SCID; hemophagocytic syndrome; thrombotic microangiopathy.

Human herpesvirus 6 (HHV-6) is a ubiquitous DNA virus that is the causative agent of roseola infantum, and infects individuals by 3 years of age [1]. After primary infection, HHV-6 establishes a latent state in the host. There are 2 distinct species, HHV-6A and HHV-6B. Most HHV-6 infections are caused by HHV-6B, whereas HHV-6A is less common. Chromosomally integrated HHV-6 (ciHHV-6) is the state in which HHV-6 (HHV-6A or HHV-6B) is integrated into the host germline genome, and it is transmitted vertically in a Mendelian manner. Although ciHHV-6 affects about 1% of the general population, it is generally considered to be a nonpathogenic condition. However, it is unclear whether ciHHV-6 can be activated with pathogenic effects on the human body [2].

Severe combined immunodeficiency (SCID) is a group of genetic disorders that result in a combined absence of T- and B-cell immunity. It is characterized by life-threatening infections during the first year of life unless treated, usually with hematopoietic stem cell transplantation (HSCT). X-linked severe combined immunodeficiency (X-SCID) arises from a mutation in the interleukin 2 receptor, gamma (*IL2RG*) gene on the X-chromosome [3]. We encountered a boy with X-SCID in whom ciHHV-6A was activated.

CASE REPORT

A 2-month-old boy was hospitalized for recurrent episodes of fever, cough, diarrhea, and failure to thrive. Upon admission, a viral infection was suspected, and supportive care did not improve his symptoms.

Twenty days after admission, mild pancytopenia (leukocyte count, 1.4×10^9/L; hemoglobin level, 78 g/L; and platelet count, 37×10^9/L) and elevated aminotransferases and ferritin were evident (aspartate aminotransferase, 448 U/L; alanine aminotransferase, 218 U/L; and ferritin, 4325 ng/mL) (Supplementary Figure 1). A bone marrow biopsy showed a hypocellular condition without dysplastic changes, as well as increased activated phagocytes. These results suggested hemophagocytic syndrome (HPS).

An immunological evaluation revealed an absence of T cells and low immunoglobulin levels. Genetic analysis identified a mutation in the *IL2RG* that was consistent with X-SCID. The patient's mother was heterozygous for the same mutation, and there was no such mutation detected in the patient's father.

A comprehensive search for a pathogen identified high levels of HHV-6 DNA (1.2×10^7 copies/μg DNA) in his peripheral blood. Antiviral treatment with ganciclovir or foscarnet did not reduce the viral load, and ciHHV-6 was suspected. We detected high levels of HHV-6 DNA in the patient's fingernails, the father's peripheral blood, and the father's hair follicles (5.9×10^5, 1.0×10^7, 1.2×10^6 copies/μgDNA, respectively).

Received 7 January 2014; accepted 9 April 2014; electronically published 6 May 2014.

Correspondence: Shuki Mizutani, MD, Department of Pediatrics and Developmental Biology, Tokyo Medical and Dental University, 1-5-45, Yushima, Bunkyo-ku, Tokyo 113-8510, Japan (skkmiz@gmail.com).

Clinical Infectious Diseases 2014;59(4):545–8

DOI: 10.1093/cid/ciu323

Fluorescence in situ hybridization analysis of the patient's fibroblasts and his father's peripheral blood mononuclear cells (PBMCs) confirmed HHV-6 integration at chromosome 22 in both individuals (Figure 1); these results suggested vertical germline transmission.

However, discontinuation of antiviral treatment led to a deterioration of the patient's HPS. Because no other pathogen was detected, activation of HHV-6 was suspected. To confirm this suspicion, we performed 3 assays that could detect viral activation despite the presence of integrated HHV-6 DNA. First, reverse transcription polymerase chain reaction (RT-PCR) was used to detect viral RNA in whole-blood samples. RT-PCR was performed on 2 HHV-6 genes, the late gene U60/66 and the immediate-early (IE) gene IE1, as described previously [5]. We detected viral RNA for both genes (4.6×10^2 copies/μg RNA for U60/66 and 5.2×10^3 copies/μg RNA for IE1). Second, immunostaining was used to detect IE antigens in a bone marrow sample taken at the time of HPS (Figure 2 and Supplementary Figure 2) [6]. Last, HHV-6A was isolated from the patient's PBMCs. It was cultured with cord blood cells and its presence confirmed by immunofluorescent staining with an anti–HHV-6 monoclonal antibody (Figure 3 and Supplementary Figure 3) [1].

Two hypotheses were postulated: Either the patient with ciHHV-6 was infected de novo with HHV-6, or HHV-6 was activated from the ciHHV-6 genome present in this patient. We performed a sequence analysis of the HHV-6 IE1 gene, as IE1 is variable and readily used to distinguish between HHV-6 variants [7]. DNA samples from isolated HHV-6A (described above), the patient's fingernails, his father's hair follicles, and laboratory strains U1102 and Z29 were amplified by PCR and sequenced. Because active HHV-6 is not present in the fingernails or hair follicles, we could amplify the original integrated HHV-6 strain from the genomes in these tissues. To our surprise, the sequences and subsequent phylogenetic analysis revealed that the isolated virus was identical to the original integrated HHV-6A strain present in both the patient and his father. Furthermore, this HHV-6A strain was unique in that it differed from all other HHV-6 strains analyzed (Supplementary Figure 4). These results suggested that the isolated HHV-6A strain originated from the activation of ciHHV-6A. Analysis of 3 other viral genes (gB, U94, and DR) confirmed these results [8, 9].

The resumption of antiviral drug treatment with prednisolone ameliorated the patient's HPS. When he reached age 7 months, the patient underwent HSCT. Antiviral drug treatment was continued during HSCT, and engraftment was achieved 14 days after transplant. After engraftment, thrombotic microangiopathy (TMA) and gastrointestinal bleeding developed. Simultaneously, the patient's HHV-6A DNA and RNA titers increased, and HHV-6A was reisolated. Anticoagulant therapy and a reduction in tacrolimus dosage gradually improved the patient's TMA. With immunological reconstruction, the patient's HHV-6A DNA and RNA titers were successfully reduced and ultimately, no HHV-6A was isolated from subsequent blood samples. The asymptomatic patient was discharged at 12 months.

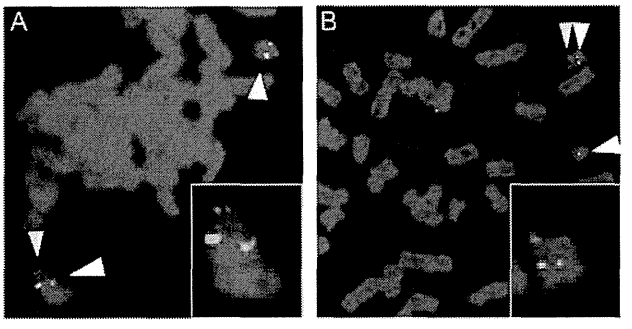

Figure 1. Integration of human herpesvirus type 6 (HHV-6) in chromosome 22 was demonstrated by fluorescence in situ hybridization analysis. Fibroblasts derived from the patient's skin (*A*) and peripheral blood mononuclear cells from the father (*B*) were cohybridized with HHV-6-specific (yellow arrow) and chromosome-22-specific probes (white arrows) [4]. HHV-6 integration in only one of the chromosome 22 alleles was shown in both materials. In sets of *A* and *B* are the enlared images of FISH data positively cohybridized with both probes.

DISCUSSION

Since the discovery of ciHHV-6 in 1993, the question of whether ciHHV-6 can be activated from its integrated state has been perpetually debated [2]. With this case report, we provide the first molecular and virological evidence of viral activation from ciHHV-6A in the human body. This evidence comprises (1) viral RNA and antigens detected in PBMCs and bone marrow, as well as HHV-6A isolated from PBMCs; (2) HHV-6A sequences integrated into the patient's and his father's genomes, which were identical to those of the isolated virus; and (3) antiviral treatment and immunological reconstruction, which were effective in treating this activated ciHHV-6A.

In an effort to understand the biological significance of ciHHV-6, active viral replication from ciHHV-6 has recently been demonstrated in vitro under specific experimental conditions [9–11]. However, only a few studies have suggested ciHHV-6 activation in vivo despite high ciHHV-6 prevalence (approximately 1%) in the general population [12–14]. Activation of ciHHV-6 in vivo has been previously reported in mothers with ciHHV-6 who passed on the infection to infants who did not have inherited ciHHV-6 [8]. Our findings are consistent with these findings, as we clearly demonstrate the activation of HHV-6A in a patient who acquired ciHHV-6 via germline transmission.

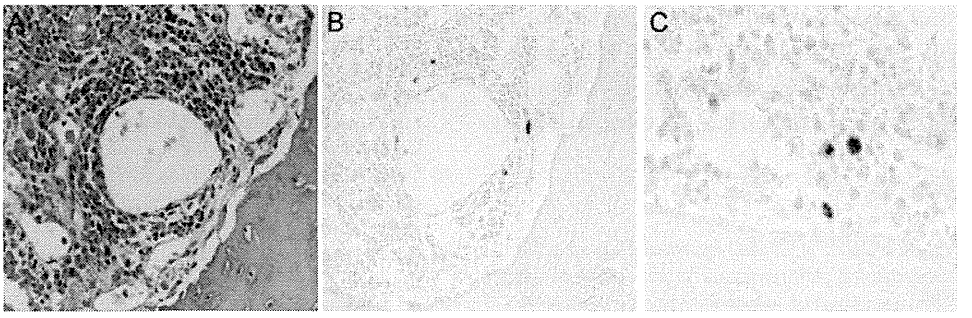

Figure 2. Histology and human herpesvirus type 6 (HHV-6) immunostaining. *A*, Hematoxylin and eosin staining of bone marrow. *B* and *C*, Immunostaining with an anti–HHV-6 antibody.

We speculate that the presence of X-SCID allowed for efficient activation of ciHHV-6A, and this phenomenon was detected with several technical strategies. Similarly, RT-PCR and virus isolation showed conversion from an HHV-6–positive status to a negative status with the patient's immunological recovery. In addition, these techniques were used to test samples taken from the patient's father. We were able to determine that he was indeed the ciHHV-6 carrier, yet he was HHV-6A negative. This suggests that X-SCID influenced the activation of ciHHV-6A. Because X-SCID prevalence is extremely low (about 0.001%), this case provides valuable insight into immunocompromised individuals and HHV-6 infection. However, the mechanism that triggered ciHHV-6A activation and replication in this patient remains to be elucidated. Further studies of patients with ciHHV-6 are required to determine what causes activation of this latent integrated virus.

The association between HHV-6 and HPS has previously been reported [15], and a link between HHV-6 and TMA has also been noted [16]. Therefore, it is possible that ciHHV-6A activation in our patient was associated with HPS and TMA. We noted that active HHV-6A infection coincided with symptom onset and the active infection was controlled with antiviral treatment. This suggests that HHV-6A is pathogenic, yet it remains to be established whether activated HHV-6A enhances underlying pathological conditions, and whether the activation of ciHHV-6A occurs in a similar fashion for all infected individuals.

Latent HHV-6 reactivation occurs in 40%–50% of recipients during HSCT, and our case report is the first to demonstrate that ciHHV-6A activation also occurs during this procedure. It is possible that the presence of X-SCID allowed for viral activation, but further studies are required to validate this hypothesis.

We have described the first case to provide molecular and virological evidence of the activation of chromosomally integrated HHV-6A in the human body. However, our report has limitations. We still do not know how virus production was triggered from a state of ciHHV-6A or how the production of the virus affected the patient's symptoms. Despite these limitations, based on this case, we hypothesize that an immunodeficient phenotype in conjunction with uncontrolled host defense systems allows the activation of ciHHV-6A. We support the recommendation that a screening program to detect ciHHV-6 in

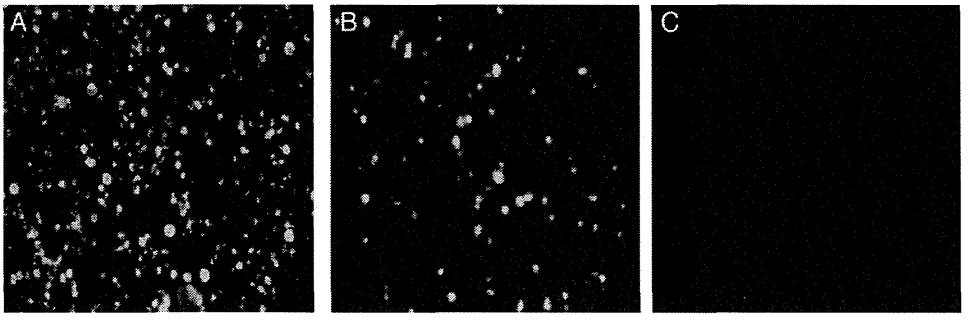

Figure 3. Immunofluorescent staining assay. *A*, Virus isolation confirmed with an anti– human herpesvirus type 6 antibody (gp116/64/54). *B*, U1102 cultured with cord blood cells (positive control). *C*, Cord blood cells alone (negative control).

transplant patients and donors be established, and recommend that ciHHV-6 patients with immunocompromised status such as primary immunodeficiency, human immunodeficiency virus infection, or organ transplantation, be monitored carefully.

Supplementary Data

Supplementary materials are available at *Clinical Infectious Diseases* online (http://cid.oxfordjournals.org). Supplementary materials consist of data provided by the author that are published to benefit the reader. The posted materials are not copyedited. The contents of all supplementary data are the sole responsibility of the authors. Questions or messages regarding errors should be addressed to the author.

Notes

Financial support. This work was supported by the Ministry of Health, Labour, and Welfare of Japan (H25 Shinko-Ippan-015 to H. Ka., H23 Nanchi-Ippan-003 and H25 Nanchitou-Menneki-Ippan-105 to T. Mo.); the Japan Society for the Promotion of Science (22590426 to N. I.); and the Ministry of Education, Culture, Sciences, and Technology in Japan (23390270 and 23390271 to T. Mo. and S. M.).

Potential conflicts of interest. All authors: No reported conflicts.

All authors have submitted the ICMJE Form for Disclosure of Potential Conflicts of Interest. Conflicts that the editors consider relevant to the content of the manuscript have been disclosed.

References

1. Yamanishi K, Shiraki K, Kondo T, et al. Identification of human herpesvirus-6 as a causal agent for exanthema subitum. Lancet **1988**; 1: 1065–7.
2. Pellett PE, Ablashi DV, Ambros PF, et al. Chromosomally integrated human herpesvirus 6: questions and answers. Rev Med Virol **2012**; 22: 144–55.
3. Sugamura K, Asao H, Kondo M, et al. The interleukin-2 receptor gamma chain: its role in the multiple cytokine receptor complexes and T cell development in XSCID. Annu Rev Immunol **1996**; 14: 179–205.
4. Isegawa Y, Mukai T, Nakano K, et al. Comparison of the complete DNA sequences of human herpesvirus 6 variants A and B. J Virol **1999**; 73: 8053–63.
5. Van den Bosch G, Locatelli G, Geerts L, et al. Development of reverse transcriptase PCR assays for detection of active human herpesvirus 6 infection. J Clin Microbiol **2001**; 39:2308–10.
6. Papanikolaou E, Kouvatsis V, Dimitriadis G, Inoue N, Arsenakis M. Identification and characterization of the gene products of open reading frame U86/87 of human herpesvirus 6. Virus Res **2002**; 89:89–101.
7. Yamamoto T, Mukai T, Kondo K, Yamanishi K. Variation of DNA sequence in immediate-early gene of human herpesvirus 6 and variant identification by PCR. J Clin Microbiol **1994**; 32:473–6.
8. Gravel A, Hall CB, Flamand L. Sequence analysis of transplacentally acquired human herpesvirus 6 DNA is consistent with transmission of a chromosomally integrated reactivated virus. J Infect Dis **2013**; 207:1585–9.
9. Arbuckle JH, Medveczky MM, Luka J, et al. The latent human herpesvirus-6A genome specifically integrates in telomeres of human chromosomes in vivo and in vitro. Proc Natl Acad Sci U S A **2010**; 107:5563–8.
10. Prusty BK, Krohne G, Rudel T. Reactivation of chromosomally integrated human herpesvirus-6 by telomeric circle formation. PLoS Genet **2013**; 9:e1004033.
11. Huang Y, Hidalgo-Bravo A, Zhang E, et al. Human telomeres that carry an integrated copy of human herpesvirus 6 are often short and unstable, facilitating release of the viral genome from the chromosome. Nucleic Acids Res **2014**; 42:315–27.
12. Kobayashi D, Kogawa K, Imai K, et al. Quantitation of human herpesvirus-6 (HHV-6) DNA in a cord blood transplant recipient with chromosomal integration of HHV-6. Transpl Infect Dis **2011**; 13:650–3.
13. Troy SB, Blackburn BG, Yeom K, Caulfield AK, Bhangoo MS, Montoya JG. Severe encephalomyelitis in an immunocompetent adult with chromosomally integrated human herpesvirus 6 and clinical response to treatment with foscarnet plus ganciclovir. Clin Infect Dis **2008**; 47: e93–6.
14. Wittekindt B, Berger A, Porto L, et al. Human herpes virus-6 DNA in cerebrospinal fluid of children undergoing therapy for acute leukaemia. Br J Haematol **2009**; 145:542–5.
15. Tanaka H, Nishimura T, Hakui M, Sugimoto H, Tanaka-Taya K, Yamanishi K. Human herpesvirus-6-associated hemophagocytic syndrome in a healthy adult. Emerg Infect Dis **2002**; 8:87–8.
16. Matsuda Y, Hara J, Miyoshi H, et al. Thrombotic microangiopathy associated with reactivation of human herpesvirus-6 following high-dose chemotherapy with autologous bone marrow transplantation in young children thrombotic microangioapathy. Bone Marrow Transplant **1999**; 24:919–23.

LIVER TRANSPLANTATION 20:391–393, 2014

LETTER FROM THE FRONTLINE

Hepatocyte Transplantation Using a Living Donor Reduced Graft in a Baby With Ornithine Transcarbamylase Deficiency: A Novel Source of Hepatocytes

Received October 29, 2013; accepted November 17, 2013.

TO THE EDITORS:

We performed hepatocyte transplantation (HT) in an 11-day-old infant with ornithine transcarbamylase deficiency (OTCD). We used cryopreserved hepatocytes prepared from remnant liver tissue, a byproduct of a hyper-reduced left lateral segment from living donor liver transplantation (LDLT). The patient exhibited hypothermia, drowsiness, and apnea at 3 days of age; these symptoms were accompanied by hyperammonemia (1940 μg/dL at maximum), although there were no abnormalities at birth or an obvious family history (Fig. 1). Further examinations confirmed that the hyperammonemia was the result of OTCD. Multimodal treatments, including alimentotherapy, medications, and continuous hemodiafiltration (CHDF), did not improve the patient's clinical state, and severe hyperammonemia attacks recurred. Because of the patient's small body size (2550 g) and the lack of an available liver donor, HT was indicated. Hepatocytes of the same blood type were chosen from an institutional repository of cryopreserved hepatocytes prepared from the remnant tissue of segment III from unrelated living donors. Thawed hepatocytes were transplanted twice at 11 and 14 days of age with a double-lumen catheter inserted into the left portal vein via the umbilical vein (Fig. 2). The amounts of transplanted hepatocytes were 7.4×10^7 and 6.6×10^7 cells/body, and the viability rates were 89.1% and 82.6%, respectively. The portal flow was kept stable at greater than 10 mL/kg/minute, and the pressure was maintained at less than 20 mm Hg during and after HT. The immunosuppressive treatment followed the same protocol used for LDLT with tacrolimus and low-dose steroids.[1] The patient was weaned from CHDF and the ventilator at 26 and 30 days of age, respectively, with a stable serum ammonia level of 40 μg/dL. The patient was ultimately discharged 56 days after HT. During the 3 months of follow-up, the baby did well with protein restriction (2 g/kg/day), medication for OTCD, and immunosuppression. No neurological sequelae related to hyperammonemia have been observed so far (Fig. 1).

DISCUSSION

For children with metabolic liver disease, HT is indicated as an alternative or bridge to liver transplantation.[2] HT is less invasive than liver transplantation and can be performed repeatedly. Limitations to the widespread application of HT include the poor availability of hepatocytes. Therefore, it is important to find new sources of high-quality hepatocytes. We previously prepared a repository of hepatocytes obtained from remnant liver tissue, a byproduct of hyper-reduced left lateral segmentectomy in LDLT.[1]

The cell donor was an unrelated volunteer with the same blood type who had previously undergone hyper-reduced left lateral segmentectomy. The main unit of segment II was used as a monosegmental liver graft for the primary recipient with end-stage liver disease, and the remnant was used to isolate hepatocytes with fully informed consent. The hepatocytes were isolated according to the collagenase perfusion method, as described elsewhere,[3] with Liberase MTF C/T GMP grade (Roche). All procedures were performed at our cell processing center according to a strictly controlled protocol based on good manufacturing practices. The total number of transplanted live hepatocytes was 1.4×10^8 cells/body; the ammonia removal rate was more than 200 fmol/cell/hour (203.4 and 265.4 fmol/cell/hour with the first and second injections, respectively). The dose was judged to be sufficiently high to obtain therapeutic effectiveness according to our theoretical background.[4]

This work was supported by a grant-in-aid from the National Center for Child Health and Development and the Highway Program for the Realization of Regenerative Medicine (Japanese Science and Technology Agency). This study protocol was approved by institutional review board in National Center for Child Health and Development (reference number 433).

Address reprint requests to Mureo Kasahara, M.D., Ph.D., National Center for Child Health and Development, 2-10-1 Okura, Setagaya-Ku, Tokyo, Japan 157-8535. Telephone: +81-3-3416-0181; FAX: +81-3-3416-2222; E-mail: kasahara-m@ncchd.go.jp

DOI 10.1002/lt.23800
View this article online at wileyonlinelibrary.com.
LIVER TRANSPLANTATION. DOI 10.1002/lt. *Published on behalf of the American Association for the Study of Liver Diseases*

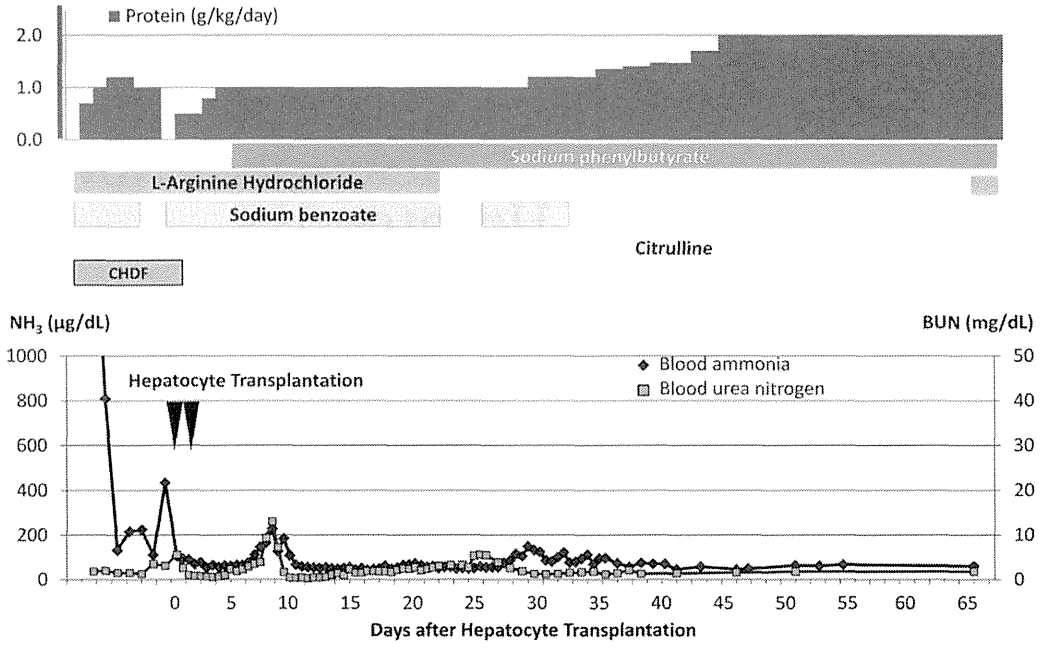

Figure. 1. Treatment schedule (top) and patient condition (bottom). The changes with time for blood ammonia and blood urea nitrogen are shown. The baby was delivered vaginally as a first child. At 3 days of age, hypothermia, low oxygen saturation, and, finally, respiratory arrest occurred. The patient was incubated and given artificial respiration. Concurrently, hyperammonemia (1940 μg/dL) was found, and continuous hemodiafiltration (CHDF) was started in addition to alimentotherapy (protein withdrawal) and medications. Whenever the administration of essential amino acids was restarted, the blood ammonia level became elevated, and at 9 days of age, despite the suspension of essential amino acid administration, the level increased up to 434 μg/dL. At 11 days of age, HT was performed for the first time, and it was performed for the second time at 14 days of age. After HT, amino acid intake was restarted along with the continuation of multimodal treatments, and blood ammonia was controlled well except for episodic increases. The patient was weaned from CHDF and the ventilator at 26 and 30 days of age, respectively, and the patient was ultimately discharged 56 days after HT.

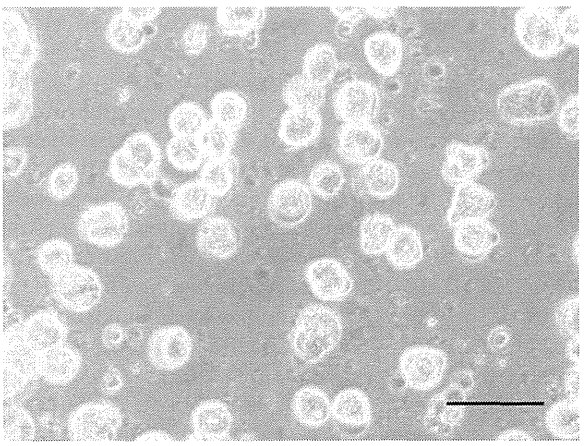

Figure. 2. Hepatocytes transplanted during the first injection. The cells showed a glazed and firm surface. The bar indicates 50 μm.

Because liver transplantation is approved as a treatment for end-stage hepatic failure, donor livers are preferentially allocated for organ transplantation and not for hepatocyte isolation. On rare occasions, the lack of appropriate donor-recipient matching (eg, infant donor livers) provides good-quality hepatocytes.[2] Fetal livers are also considered to be an alternative cell source, although ethical issues remain to be resolved. At present, we have little choice but to use marginal donor tissues, such as livers obtained from donors after cardiac death and organs with steatosis, fibrosis, or a long ischemia time. However, there are unfavorable issues related to the use of marginal donors, including low viability and vulnerability to cryopreservation. In this respect, the remnant liver tissue of hyper-reduction procedures used in LDLT has the same quality as that of left lateral segment grafts. As for availability, there are 5 cases of hyper-reduction per year at our institution on average.[5] The use of remnant liver tissues obtained from hyper-reduced LDLT procedures will, therefore, help to address the shortage of hepatocyte donors.

Shin Enosawa, D.D.S., Ph.D.
Reiko Horikawa, M.D., Ph.D.
Akiko Yamamoto, M.D.
Seisuke Sakamoto, M.D., Ph.D.
Takanobu Shigeta, M.D.
Shunsuke Nosaka, M.D., Ph.D.
Junichiro Fujimoto, M.D., Ph.D.
Atsuko Nakazawa, M.D., Ph.D.
Akito Tanoue, M.D., Ph.D.
Kazuaki Nakamura, Ph.D.
Akihiro Umezawa, M.D., Ph.D.
Yoichi Matsubara, M.D., Ph.D.
Akira Matsui, M.D., Ph.D.
Mureo Kasahara, M.D., Ph.D.
National Center for Child Health and Development, Tokyo, Japan

REFERENCES

1. Kasahara M, Kaihara S, Oike F, Ito T, Fujimoto Y, Ogura Y, et al. Living-donor liver transplantation with monosegments. Transplantation 2003;76:694-696.
2. Meyburg J, Das AM, Hoerster F, Lindner M, Kriegbaum H, Engelmann G, et al. One liver for four children: first clinical series of liver cell transplantation for severe neonatal urea cycle defects. Transplantation 2009;87:636-641.
3. Alexandrova K, Griesel C, Barthold M, Heuft HG, Ott M, Winkler M, et al. Large-scale isolation of human hepatocytes for therapeutic application. Cell Transplant 2005; 14:845-853.
4. Enosawa S, Yuan W, Douzen M, Nakazawa A, Omasa T, Fukuda A, et al. Consideration of a safe protocol for hepatocyte transplantation using infantile pigs. Cell Med 2012;3:13-18.
5. Kanazawa H, Sakamoto S, Fukuda A, Uchida H, Hamano I, Shigeta T, et al. Living-donor liver transplantation with hyperreduced left lateral segment grafts: a single-center experience. Transplantation 2013;95: 750-754.

LIVER TRANSPLANTATION 20:1127–1137, 2014

ORIGINAL ARTICLE

Hepatocytes Buried in the Cirrhotic Livers of Patients With Biliary Atresia Proliferate and Function in the Livers of Urokinase-Type Plasminogen Activator–NOG Mice

Hiroshi Suemizu,[1]* Kazuaki Nakamura,[3]* Kenji Kawai,[2] Yuichiro Higuchi,[1] Mureo Kasahara,[4] Junichiro Fujimoto,[5] Akito Tanoue,[3] and Masato Nakamura[6]

[1]Biomedical Research Department, and [2]Pathology Research Department, Central Institute for Experimental Animals, Kanagawa, Japan; [3]Department of Pharmacology, [4]Department of Transplant Surgery, and [5]Clinical Research Center, National Center for Child Health and Development, Tokyo, Japan; and [6]Department of Pathology and Regenerative Medicine, Tokai University School of Medicine, Kanagawa, Japan

The pathogenesis of biliary atresia (BA), which leads to end-stage cirrhosis in most patients, has been thought to inflame and obstruct the intrahepatic and extrahepatic bile ducts. BA is not believed to be caused by abnormalities in parenchymal hepatocytes. However, there has been no report of a detailed analysis of hepatocytes buried in the cirrhotic livers of patients with BA. Therefore, we evaluated the proliferative potential of these hepatocytes in immunodeficient, liver-injured mice [the urokinase-type plasminogen activator (uPA) transgenic NOD/Shi-scid IL2rγnull (NOG); uPA-NOG strain]. We succeeded in isolating viable hepatocytes from the livers of patients with BA who had various degrees of fibrosis. The isolated hepatocytes were intrasplenically transplanted into the livers of uPA-NOG mice. The hepatocytes of only 3 of the 9 BA patients secreted detectable amounts of human albumin in sera when they were transplanted into mice. However, human leukocyte antigen–positive hepatocyte colonies were detected in 7 of the 9 mice with hepatocyte transplants from patients with BA. We demonstrated that hepatocytes buried in the cirrhotic livers of patients with BA retained their proliferative potential. A liver that was reconstituted with hepatocytes from patients with BA was shown to be a functioning human liver

Additional Supporting Information may be found in the online version of this article.

Abbreviations: 5-CF, 5-carboxyfluorescein; 5-CFDA, 5(6)-carboxyfluorescein diacetate; αSMA, alpha smooth muscle actin; ABC, adenosine triphosphate–binding cassette; ALB, albumin; BA, biliary atresia; BC, bile canaliculus; CFDA, 5-carboxyfluorescein diacetate; CYP, cytochrome P450; GAPDH, glyceraldehyde-3-phosphate dehydrogenase; hALB, human albumin; H&E, hematoxylin and eosin; HIF, high intrinsic fluorescence; HLA, human leukocyte antigen; IF, intrinsic fluorescence; LT, liver transplantation; MRP2, multidrug resistance–associated protein 2; ND, not detected by an enzyme-linked immunosorbent assay; NGS, normal goat serum; NMS, normal mouse serum; NR1, nuclear receptor subfamily 1; NRS, normal rabbit serum; PELD, Pediatric End-Stage Liver Disease; PI, propidium iodide; SLC, solute carrier family; UGT, uridine diphosphate glucuronosyltransferase; uPA, urokinase-type plasminogen activator; VIM, vimentin.

The authors report no conflicts of interest.

Hiroshi Suemizu was the primary experimenter, performed all transplants, analyzed the liver-reconstituted mice, and wrote the article. Kazuaki Nakamura, Mureo Kasahara, Junichiro Fujimoto, and Akito Tanoue performed all isolations of human hepatocytes and managed all the clinical samples. Kenji Kawai provided all the tissue histology. Yuichiro Higuchi analyzed the liver-reconstituted mice. Masato Nakamura provided overall project planning and coordination.

This work was supported in part by Grants-in-Aid for Scientific Research to Hiroshi Suemizu (21240042) and Akito Tanoue (23300162) from the Japan Science and Technology Agency.

*These authors contributed equally to this work.

Address reprint requests to Hiroshi Suemizu, Ph.D., Biomedical Research Department, Central Institute for Experimental Animals, 3-25-12 Tonomachi, Kawasaki-Ku, Kawasaki, Kanagawa 210-0821, Japan. Telephone: +81-44-201-8530; FAX: +81-44-201-8541 or +81-44-201-8511; E-mail: suemizu@ciea.or.jp or nogmouse@ciea.or.jp

DOI 10.1002/lt.23916
View this article online at wileyonlinelibrary.com.
LIVER TRANSPLANTATION.DOI 10.1002/lt. *Published on behalf of the American Association for the Study of Liver Diseases*

with a drug-metabolizing enzyme gene expression pattern that was representative of mature human liver and biliary function, as ascertained by fluorescent dye excretion into the bile canaliculi. These results imply that removing the primary etiology via an earlier portoenterostomy may increase the quantity of functionally intact hepatocytes remaining in a cirrhotic liver and may contribute to improved outcomes. *Liver Transpl 20:1127-1137, 2014.* © 2014 AASLD.

Received January 2, 2014; accepted May 10, 2014.

Biliary atresia (BA), the most common pediatric cholestatic disease, is caused by the progressive fibro-obliterative obstruction of the extrahepatic and intrahepatic bile ducts within the first few weeks of life.[1,2] The current surgical treatment is sequential. In the first few weeks of life, a Kasai portoenterostomy is performed to bypass the obstructed extrahepatic bile ducts and restore the biliary flow.[3] Approximately 20% of all patients who undergo portoenterostomy during infancy survive into adulthood with their native liver.[2,4] In general, it is advantageous to perform portoenterostomy as early after birth as possible to optimize the chance of success.[5] Patients who fail to undergo portoenterostomy experience a gradual deterioration of liver function and develop progressive fibrosclerosis; after the initial successful establishment of bile flow, liver transplantation (LT) is the only treatment option. Although several etiologies of BA have been postulated, the precise pathogenesis of BA remains unknown. Some factors that might contribute to its development are genetic, infective, inflammatory, and toxic insults.[1] In most cases, BA is associated with an intensive inflammatory infiltrate; this knowledge led us to the conjecture that BA results from an infectious or autoimmune destruction of the bile ducts. For example, the infection of newborn mice with the Rhesus rotavirus results in a BA-like disease.[6-8] Meanwhile, hepatocytes from patients with BA have not been thought to be involved in the development of chronic obstructive cholestasis. We and other groups have developed mice with humanized livers in which the liver is reconstituted with human hepatocytes so that in vivo drug metabolism and liver regeneration can be studied.[9-11] Therefore, the aims of this study were to evaluate the in vivo proliferative potential and functional properties of hepatocytes buried in the cirrhotic livers of BA patients.

MATERIALS AND METHODS

Specimens from the National Research Institute for Child Health and Development were collected in a standardized manner with the permission of the patients' families.

Animals

All mouse studies were conducted in strict accordance with *Guide for the Care and Use of Laboratory Animals* from the Central Institute for Experimental Animals. All experimental protocols were approved by the animal care committee of the Central Institute for Experimental Animals (permit number 11029A). All surgeries were performed under isoflurane anesthesia, and all efforts were made to minimize animal suffering. All studies using mouse tissue with transplanted human cells were approved by the ethics and biosafety committee of the National Research Institute for Child Health and Development and the Central Institute for Experimental Animals. The urokinase-type plasminogen activator (uPA) transgenic NOD/Shi-scid IL2rγnull (NOG); uPA-NOG strain[11] was maintained through the breeding of a female uPA-NOG hemizygote with a male homozygote. The zygosity of the *uPA* transgene was presumed from the degree of liver damage, which was examined through the determination of the serum levels of alanine aminotransferase with a Fuji DRI-CHEM 7000 clinical biochemical analyzer (Fujifilm Corp., Tokyo, Japan). The uPA-NOG mice with serum alanine aminotransferase activity greater than 150 U/L were selected as homozygotes and were then used as transplant recipients.

Isolation of Hepatocytes From the Livers of Patients With BA

The entire experimental protocol was approved by the ethics and research committee of the National Center for Child Health and Development. Written informed consent was obtained in each case. Except for the pieces of liver tissue that were used as pathological specimens, the enucleated diseased livers from the transplant recipients were discarded. The human hepatocytes used in this study were procured from liver tissue removed from BA patients who met the diagnostic criteria [Pediatric End-Stage Liver Disease (PELD) score[12] $\geq$ 6 points] for LT operations. The levels of fibrosis were categorized according to the following criteria: (I) mild (portal fibrous expansion to bridging fibrosis involving $\leq$50% of portal tracts), (II) moderate (bridging fibrosis involving >50% of portal tracts), and (III) severe (bridging fibrosis involving >50% of the portal tracts with nodular architectural changes).[13] Patient 141, who had grade III fibrosis and a PELD score of 0, had portopulmonary syndrome (intrapulmonary shunting). The shunt ratio, calculated with technetium-99m macroaggregated albumin (ALB) scintigraphy, was 16.8%, which indicated a relatively mild shunt. The hepatocytes were isolated from the resected liver tissue through the 2-step collagenase perfusion[14] of the liver samples, as described previously.[15] Hepatic parenchymal cells were isolated with low-speed centrifugation (50*g*). Cell numbers and viability were assessed with trypan blue exclusion.[16]

Flow Cytometry Analysis

The hepatocytes were stained with 1 mg/mL propidium iodide (PI; Sigma-Aldrich Co. LLC, St. Louis, MO), which stains dead cells. The intensity of 502-nm fluorescence was measured as intrinsic fluorescence (IF). Flow cytometry data were collected with a FACSCanto analyzer and BD FACSDiva software (BD Biosciences, Franklin Lakes, NJ). The data were analyzed with the FlowJo program (Tree Star, Inc., Ashland, OR).

Transplantation of Hepatocytes Into uPA-NOG Mice

Hepatocytes from patients with BA and commercially available cryopreserved human hepatocytes from a 4-year-old female (NHEPS, Lonza, Walkersville, MD) were used as donor cells. Young (8-week-old) male uPA-NOG mice were used as the recipients of the human hepatocytes. One million viable hepatocytes were injected intrasplenically via a Hamilton syringe with a 26-G needle. The successful engraftment of the human hepatocytes was evaluated through the measurement of the blood level of human albumin (hALB) with an hALB enzyme-linked immunosorbent assay quantitation kit (Bethyl Laboratories, Montgomery, TX) according to the manufacturer's protocol. The replacement index, which was the percentage of human donor hepatocytes in the recipient liver, was estimated according to the hALB concentration in chimeric mice.[17]

Histology and Immunohistochemistry

The tissues were fixed with 4% (vol/vol) phosphate-buffered formalin (Mildform, Wako Pure Chemical Industries, Ltd., Osaka, Japan), and 5-μm paraffin-embedded sections were stained with Azan-Mallory staining reagents (Muto Pure Chemicals, Tokyo, Japan) to visualize the collagen and muscle fibers and with hematoxylin and eosin (H&E). Some sections were autoclaved for 10 minutes in a target retrieval solution [0.1 M citrate buffer (pH 6.0) and 1 mM ethylene diamine tetraacetic acid (pH 9.0)] and were then equilibrated at room temperature for 20 minutes. Monoclonal mouse anti–human leukocyte antigen (anti-HLA) class I (A-C) antibodies (clone EMR8-5, Hokudo, Sapporo, Japan; 1:2000),[18] polyclonal goat anti-human ALB antibodies (Bethyl Laboratories; 1:1500), polyclonal rabbit anti-cytochrome P450 3A4 (CYP3A4) antibodies (Abcam, Inc., Cambridge, MA; 1:500), monoclonal mouse anti-human Ki-67 antigen antibodies (clone MIB-1; Dako Denmark A/S; 1:50),[19] monoclonal mouse anti-human multidrug resistance–associated protein 2 (MRP2) antibodies (clone M2 III-6, Millipore, Billerica, MA; 1:100),[20] monoclonal rabbit anti-vimentin (anti-VIM) antibodies (clone SP20, Nichirei Bioscience, Tokyo, Japan; 1:1500),[21] and monoclonal rabbit anti–alpha smooth muscle actin (anti-αSMA) antibodies (clone 1A4, Leica Microsystems, Tokyo, Japan; 1:200)[22] were used as primary antibodies. Normal mouse serum (NMS), normal goat serum (NGS), and normal rabbit serum (NRS) were used as negative controls for immunostaining. For bright-field immunohistochemistry, the antibodies for mouse, goat, and rabbit immunoglobulin were visualized with amino acid polymer/peroxidase complex–labeled antibodies [Histofine Simple Stain MAX PO (M, G, and R), Nichirei Bioscience) and a Bond Polymer Refine Detection system (Leica Microsystems) with a diaminobenzidine substrate [Dojindo Laboratories, Kumamoto, Japan; 0.2 mg/mL 3,3′-diaminobenzidine tetrahydrochloride, 0.05 M tris(hydroxymethyl)-aminomethane with hydrochloric acid (pH 7.6), and 0.005% hydrogen peroxide]. The sections were counterstained with hematoxylin. Hepatic biliary obstructions were examined with Hall's bilirubin staining method.[23] The images were captured under an Axio Imager upright microscope (Carl Zeiss, Thornwood, NY) equipped with AxioCam HRm and AxioCam MRc5 charge-coupled device cameras (Carl Zeiss).

Real-Time Quantitative Reverse-Transcription Polymerase Chain Reaction for Drug Metabolism–Related Gene Expression

The total cellular RNA was isolated from the livers with an RNeasy mini kit (Qiagen K.K.). Complementary DNA was synthesized with a high-capacity complementary DNA reverse transcription kit (Applied Biosystems, Foster City, CA) with random hexamers. TaqMan gene expression master mix and TaqMan gene expression assays (Applied Biosystems) were used for the real-time quantitative polymerase chain reactions; amplifications were performed with an ABI-Prism 7000 sequence detection system (Applied Biosystems). The comparative threshold cycle (Ct) method was used to determine the relative ratio of the gene expression for each gene, which was corrected with human glyceraldehyde-3-phosphate dehydrogenase (GAPDH) and referenced to the RNA extracted from donor hepatocytes. The TaqMan assay numbers are listed in Table 1.

Biliary Excretion Test With 5(6)-Carboxyfluorescein Diacetate (5-CFDA)

The ester precursor of 5-carboxyfluorescein (5-CF), 5(6)-carboxyfluorescein diacetate (5-CFDA; 0.5 nmol; Sigma-Aldrich), was injected intravenously into the mouse tail vein. Ten minutes after the 5-CFDA injection, the liver was perfused with 50 nmol/L 5-CFDA for 3 minutes, and the liver was then embedded in an optimum cutting temperature (O.C.T.) compound (Sakura Finetek Japan Co., Ltd., Tokyo, Japan) and frozen in liquid nitrogen. Ten-micrometer-thick serial frozen sections were prepared and air-dried. The 5-CF fluorescent signals were captured with an Axio Imager upright microscope (Carl Zeiss) equipped with AxioCam HRm and AxioCam MRc5 charge-coupled device cameras (Carl Zeiss). After the microfluorographs were taken, the tissue sections were fixed and rehydrated sequentially in decreasing concentrations of ethanol and water, and this was followed by immunohistochemical staining for MRP2. Sections were counterstained with

TABLE 1. TaqMan Probe Information

Gene Name	Gene Description	TaqMan Assay Number
GAPDH	Glyceraldehyde-3-phosphate dehydrogenase	Hs99999905_m1
ALB	Albumin	Hs99999922_s1
CYP1A1	Cytochrome P450, family 1, subfamily A, polypeptide 1	Hs00153120_m1
CYP1A2	Cytochrome P450, family 1, subfamily A, polypeptide 2	Hs00167927_m1
CYP2A6	Cytochrome P450, family 2, subfamily A, polypeptide 6	Hs00868409_s1
CYP2B6	Cytochrome P450, family 2, subfamily B, polypeptide 6	Hs03044634_m1
CYP2C8	Cytochrome P450, family 2, subfamily C, polypeptide 8	Hs00258314_m1
CYP2C9	Cytochrome P450, family 2, subfamily C, polypeptide 9	Hs00426397_m1
CYP2C18	Cytochrome P450, family 2, subfamily C, polypeptide 18	Hs00426400_m1
CYP2C19	Cytochrome P450, family 2, subfamily C, polypeptide 19	Hs00426380_m1
CYP2D6	Cytochrome P450, family 2, subfamily D, polypeptide 6	Hs00164385_m1
CYP2E1	Cytochrome P450, family 2, subfamily E, polypeptide 1	Hs00559368_m1
CYP3A4	Cytochrome P450, family 3, subfamily A, polypeptide 4	Hs00430021_m1
CYP3A5	Cytochrome P450, family 3, subfamily A, polypeptide 5	Hs00241417_m1
UGT1A1	Uridine diphosphate glucuronosyltransferase 1 family, polypeptide A1	Hs02511055_s1
UGT2B15	Uridine diphosphate glucuronosyltransferase 2 family, polypeptide B15	Hs00870076_s1
ABCB1	Adenosine triphosphate–binding cassette, subfamily B (MDR/TAP), member 1	Hs00184500_m1
ABCB11	Adenosine triphosphate–binding cassette, subfamily B (MDR/TAP), member 11	Hs00184824_m1
ABCC2	Adenosine triphosphate–binding cassette, subfamily C (CFTR/MRP), member 2	Hs00166123_m1
ABCG2	Adenosine triphosphate–binding cassette, subfamily G (WHITE), member 2	Hs01053790_m1
SLC22A1	Solute carrier family 22 (organic cation transporter), member 1	Hs00427552_m1
SLC22A7	Solute carrier family 22 (organic anion transporter), member 7	Hs00198527_m1
SLC22A9	Solute carrier family 22 (organic anion transporter), member 9	Hs00971064_m1
NR1H4	Nuclear receptor subfamily 1, group H, member 4	Hs00231968_m1
NR1I2	Nuclear receptor subfamily 1, group I, member 2	Hs00243666_m1
NR1I3	Nuclear receptor subfamily 1, group I, member 3	Hs00901571_m1

hematoxylin. Another tissue section was fixed in 4% paraformaldehyde, and this was followed by immunofluorescent staining with monoclonal mouse anti-HLA class I (A-C) antibodies, a streptavidin/Texas Red–labeled secondary antibody (GE Healthcare Bio-Sciences), and H&E. Commercially available cryopreserved human hepatocytes (normal hepatocytes) and cells from the HCT 116 line (American Type Culture Collection, Manassas, VA), a human colorectal carcinoma cell line that easily engrafts and forms tumor cell colonies in NOG mouse livers,[24] were used as positive and negative controls for the formulation of the bile canaliculus (BC) network.

Statistical Analyses

Group comparisons were performed with the Student *t* test for independent samples. *P* values less than 0.05 were considered significant (Prism 5, GraphPad Software, Inc., La Jolla, CA).

RESULTS

Engraftment of Hepatocytes From Patients With BA in uPA-NOG Mouse Livers

Using liver failure immunodeficient mouse models, we first evaluated the regenerative potential of the residual hepatocytes buried in the cirrhotic livers of patients with BA.[11] We succeeded in isolating viable hepatocytes from the livers of 9 BA patients with various degrees of fibrosclerosis (Table 2 and Fig. 1A). The typical gross morphology of a liver from a patient with BA is shown in Fig. 1B. There was no significant difference ($P = 0.45$) between the cell yields from patients with grade II fibrosis (2.3 ± 1.6 million cells per gram of liver, $n = 3$) and patients with grade III fibrosis (3.8 ± 4.2 million cells per gram of liver, $n = 6$; Fig. 1C). The cell viability was not significantly different ($P = 0.81$) between patients with grade II fibrosis ($76.7\% \pm 16.0\%$, $n = 3$) and patients with grade III fibrosis ($73.3\% \pm 23.0\%$, $n = 6$; Fig. 1D). The isolated hepatocytes were analyzed with flow cytometry (Fig. 1D). Because the IF signal of the hepatocytes from patients with BA was not increased in comparison with normal hepatocytes, it did not seem that bile accumulated within the hepatocytes, even in the patients with BA. The viable and engraftable hepatic parenchymal cells seemed to be present in the high intrinsic fluorescence (HIF) fraction; these cells had a very large cell mass and a complicated internal structure because the percentage of the HIF fraction correlated positively with the engraftability of the hepatocytes, which was based on the plasma concentration of hALB ($r^2 = 0.8784$; Fig. 1E, right). However, the cell viability did not show a direct correlation with the plasma concentration of hALB ($r^2 = 0.0515$; Fig. 1E, center) or the percentage of the HIF fraction ($r^2 = 0.0064$; Fig. 1E, left). The isolated hepatocytes were intrasplenically transplanted into uPA-NOG mice. Successful engraftment was evaluated in terms of the detection of hALB in the mouse serum

TABLE 2. Engraftment of Hepatocytes Derived From Patients With BA in uPA-NOG Mouse Livers

Patient Information							Experimental Condition and Summarized Results				
				Isolated Hepatocytes					Animals With Engraftment		
Number	Age	Sex	Fibrosis Level	PELD Score	Cells/g of Liver	Viability (%)	HIF (%)	Condition*	Cell Dose (Cells/Mouse)	HLA-Positive Colony [n/N (%)]†	hALB [n/N (μg/mL)]
80	10 months	Female	II	20	1.2×10^6	66	9.0	A	1.0×10^6	5/5 (100)	5/5 (230-875)
								B	1.0×10^6	4/4 (100)	1/4 (280)
								C	1.0×10^6	4/4 (100)	1/4 (38)
86	7 months	Female	II	35	1.5×10^6	95	4.8	A	1.0×10^6	2/2 (100)	1/2 (35)
								B	1.0×10^6	2/4 (50)	1/4 (105)
153	8 months	Male	II	9	4.1×10^6	69	1.3	B	1.0×10^6	2/3 (67)	0/3 (ND)
105	5 months	Female	III	13	1.2×10^7	83	8.5	B	1.0×10^6	4/4 (100)	4/4 (49-294)
133	6 months	Female	III	15	6.9×10^4	33	9.2	B	2.0×10^5	0/1 (0)	0/1 (ND)
141	12 years	Female	III	0	3.0×10^6	93	4.8	B	1.0×10^6	1/1 (100)	0/1 (ND)
149	8 months	Female	III	14	3.4×10^6	67	0.8	B	1.2×10^6	3/3 (100)	0/3 (ND)
151	5 months	Female	III	10	1.4×10^6	69	5.0	B	1.0×10^6	3/4 (75)	0/4 (ND)
154	6 months	Female	III	14	3.1×10^6	95	4.2	B	1.0×10^6	0/1 (0)	0/1 (ND)
77	32 years	Male	Normal	—	2.0×10^6	88	25.5	C	1.0×10^6	5/5 (100)	5/5 (35-1516)

*The conditions were as follows: (A) fresh hepatocytes (within the first 6 hours after isolation), (B) chilled hepatocytes (stored at 4°C for more than 16 hours and up to 24 hours), and (C) cryopreserved hepatocytes.
†Hepatocyte colonies that contained more than 20 HLA-positive cells in the cross-sections.

and the appearance of HLA-positive hepatocyte colonies in the liver tissue (Fig. 1F). Although detectable amounts of secreted hALB were found only in the sera of mice that had received hepatocyte transplants from 3 of the 9 BA patients, HLA-positive hepatocyte colonies were detected as a result of 7 of the 9 hepatocyte transplants from patients with BA.

The expression of drug-metabolizing enzymes, a marker of a fully matured liver, was analyzed with real-time quantitative polymerase chain reaction. Livers reconstituted with hepatocytes from 2 different patients with BA (patients 80 and 105) and commercially available cryopreserved hepatocytes (NHEPS) were then examined. The relative gene expression profiles of hepatocytes from patients with BA were similar to those of NHEPS hepatocytes (Fig. 1G). The expression levels of most of the genes were higher in the reconstituted livers versus the donor hepatocytes (Fig. 1H).

Next, we examined the expression of ALB, a major functional marker of biosynthesis in the liver, via immunohistochemical staining with human-specific antibodies in hepatocytes originating from patients with BA (Fig. 2A, top and middle). This hepatic lineage marker protein was expressed within the human hepatocyte colonies in the reconstituted-liver mice at levels comparable to those of the liver reconstituted with cryopreserved normal hepatocytes (patient 77; Fig. 2A, bottom). The expression of CYP3A4, which is the main drug-metabolizing enzyme found in the liver, was also observed within the colonies consisting of both hepatocytes from patients with BA (Fig. 2A, top and middle) and normal hepatocytes (Fig. 2A, bottom), but it did not show the zonal distribution observed in the fully reconstituted uPA-NOG liver with NHEPS hepatocytes (Fig. 2B). Most human hepatocytes originating from the patients with BA were present as small foci that appeared to grow by clonal expansion within the uPA-NOG mouse livers. This growth was quite similar to that of normal hepatocytes from patient 77. In addition, immunohistochemical nuclear staining of serial sections of the mouse livers with an antibody (MIB-1) against the human Ki-67 antigen[25,26] revealed that the proliferative potential of the hepatocytes from the patients with BA was preserved, as evidenced by the nuclear staining of the hepatocytes located at the edges of human hepatocyte colonies (Fig. 2A, top and middle). NGS, NRS, and NMS (nonimmune), which corresponded to the host animals in which anti-ALB, anti-CYP3A4, and anti–Ki-67 antibodies, respectively, were prepared, did not react with either human or mouse hepatocytes (Fig. 2C). The hepatocyte colonies derived from the patients with BA were not stained by Azan-Mallory staining (Fig. 2A, top and middle).

Functional Integrity of Partially Humanized Livers

We confirmed the expression of MRP2 proteins on the plasma membranes of hepatocytes in both the livers of patients with BA and the partially humanized livers repopulated with hepatocytes from patients with BA